Active Climate Control

by

Joseph Warrington (PEM)

Fourth-year undergraduate project in Group F, 2007/2008

"I hereby declare that, except where specifically indicated, the work submitted herein is my own original work."

..... *J. Warrington, 28th May 2008*

Page count (excluding title page and Technical Abstract): 50

Word count: 11,378

Active Climate Control
Technical Abstract

Climatologists have reached virtual unanimity in judging humans responsible for a severe and growing threat to the stability of the earth's climate. The mechanisms by which anthropogenic greenhouse gas (GHG) emissions bring about detrimental consequences such as temperature increases and ocean acidification are now well-understood, and the solutions to these problems represent arguably mankind's greatest challenge.

These solutions can be of two kinds. Firstly diplomatic agreements can be made with the aim of reducing GHG emissions markedly over the course of this century. Although some progress is being made on this front, many argue that an investment of a second kind - in an active climate control (ACC) scheme - will be necessary in order to prevent catastrophe. Virtually everyone agrees that the cost of a 'business-as-usual' scenario would be far higher than that of taking positive action to counteract climate change.

Many predictions of warming over the next 100 to 200 years, based on complex three-dimensional circulation models of the climate, have been made and publicised. Despite the apparent detail in these models, there is often conflict between the predictions. The motivation for this project has therefore been that of any engineer: to reduce an extremely complex system down to a well-chosen approximate model in order to extract the basic characteristics of the system adequately but efficiently. With that achieved, the aim is not to use control theory to judge how best to control the climate in the face of the changes described above; this is something that has not been applied before to simplified climate models.

A box model of the climate system has been developed. It is divided into four boxes (reservoirs) for the thermal cycle, with flows between them representing the major geophysical heat transfers, and four boxes for the carbon cycle, with carbon flows between these. The thermal cycle model is based on a paper by Harvey and Schneider; the carbon cycle model is based on a review of several papers and books. The flows between reservoirs in both cycles are coupled so that heat transfers may also be functions of carbon reservoir levels, and vice versa.

The model described above is encapsulated in a matrix equation, the lines of which represent conservation laws for the flows between reservoirs. This equation can include as inputs any anthropogenic effects we wish to study: fossil fuel burning (FFB), solar dimming, deforestation, carbon sequestration etc. The nonlinear functions controlling

the flow rates between the reservoirs are linearised about the equilibrium state, which was taken to be the state of the pre-industrial climate, even though technically the climate has never been in equilibrium for any sustained period of time. This gives a linear time-invariant model of the familiar type $\dot{\mathbf{x}} = A\mathbf{x} + B\mathbf{u}$. This linearised model has been validated by comparing its forcing responses to those from literature. Those responses of the model that are tested are found to behave similarly to the reference sources, which suggests the 'engineering' reduction made has largely been a successful one.

The model has been developed such that ACC schemes can be simulated and their consequences discussed. Many ACC schemes have been proposed since the global warming problem became apparent. These proposals include carbon sequestration; seeding the ocean surface with nutrients in order to soak up carbon by promoting biological growth; pumping nutrient-rich deep seawater to the surface for the same effect; placing a large shield, or cloud of small shields, in space to block part of the earth's sunlight; or encouraging cloud formation by spraying particles into the air to act as nucleation sites.

The solar dimming (space shield) option has been studied in most detail here. Two feedback control schemes are presented. In the first, the dimming input is uniquely determined by setting the time derivative of atmospheric temperature to zero at all times. Although this holds temperature constant for any rate of solar dimming, it cannot compensate for an initial temperature offset. Also, if there is any error in the model then temperature error accumulates over time. In the second scheme, a linear quadratic regulator (LQR) is implemented. It is shown that if there is no FFB input then temperatures can be regulated to pre-industrial conditions in reasonable time. In the presence of continued FFB input, it is shown that the scheme fails but that integral feedback can be used to regulate the atmospheric temperature to its pre-industrial value. Parameters for the LQ regulator and the integral feedback are chosen so that the scheme remains practical while delivering cooling in reasonable time.

Both control schemes show that a steady-state dimming of about 1.5% of incident solar radiation is required to offset emissions of 5 Gt yr^{-1}. This compares well with similar predictions in literature. The second scheme suggests that blocking a little more than 2% in the short term would be beneficial until the cooling effect has permeated the oceans. However, the major drawback of solar dimming is that it has almost no effect on the carbon cycle, as confirmed by these simulations. Therefore, dimming does nothing to prevent effects such as ocean acidification.

Other control schemes have been investigated briefly, suggesting that either seeding the ocean with nutrients or carbon sequestration would be successful in limiting warming.

Contents

1 Introduction **3**

1.1 Background 3

1.2 Motivation 4

1.3 Classification of Climate Models 5

1.4 Project Objectives 6

2 Model Development **7**

2.1 Model Outline 7

2.1.1 Thermal Cycle 8

2.1.2 Carbon Cycle 8

2.2 Modelling the Thermal Cycle 9

2.2.1 Choice of Reservoirs 9

2.2.2 Heat Transfer Processes 10

2.3 Modelling the Carbon Cycle 14

2.3.1 Choice of Reservoirs 14

2.3.2 Carbon Transfer Processes 14

2.4 Coupling the Thermal and Carbon Cycles 17

2.4.1 The Greenhouse Effect 17

2.4.2 The Effect of Global Warming on the Thermohaline Current . . . 18

2.5 Time Invariance 18

2.6 Model Limitations 19

3 The Climate as a Control System **19**

3.1 State Space Realisation 19

3.2 Linearisation 20

3.3 Stability Analysis 22

3.4 Thermal Cycle Validation 22

3.5 Carbon Cycle Validation 23

3.6 Equilibrium Conditions 24

4 Responses to External Forcing **25**

4.1 Solar Forcing 25

4.1.1 Effect of Carbon Feedbacks 25

4.2 Anthropogenic Carbon Emissions 26

4.2.1 Emissions Scenarios 26

4.2.2 Short-term Response 27

4.3 Deforestation 27

5 About ACC Schemes **28**

5.1 Recently-discussed Countermeasures 28

5.2 Cost Functions for ACC Schemes 29

5.3 Countermeasures as Model Inputs 30

6 Solar Dimming **31**

6.1 Back-computing the Control Input 31

6.2 LQR Control 34

6.2.1 Temperature Regulation as an LQR Problem 34

6.2.2 Solar Dimming for Temperature Regulation 34

6.3 Effect of uncertainty 36

7 Other ACC Schemes **38**

7.1 Seawater Pumping 38

7.2 Carbon Sequestration 39

8 Discussion **40**

8.1 Conclusions 40

8.2 Future Work 41

9 Appendix **43**

10 Glossary and Abbreviations **47**

References **48**

1 Introduction

1.1 Background

Climatologists have reached virtual unanimity[1] in judging humans responsible for a severe and growing threat to the stability of the earth's climate. The mechanisms by which anthropogenic greenhouse gas (GHG) emissions bring about detrimental consequences such as temperature increases and ocean acidification are now well-understood, and the solutions to these problems represent arguably mankind's greatest challenge. Fig. 1 shows the most famous and concerning trends of atmospheric CO_2 concentrations and temperatures.[2]

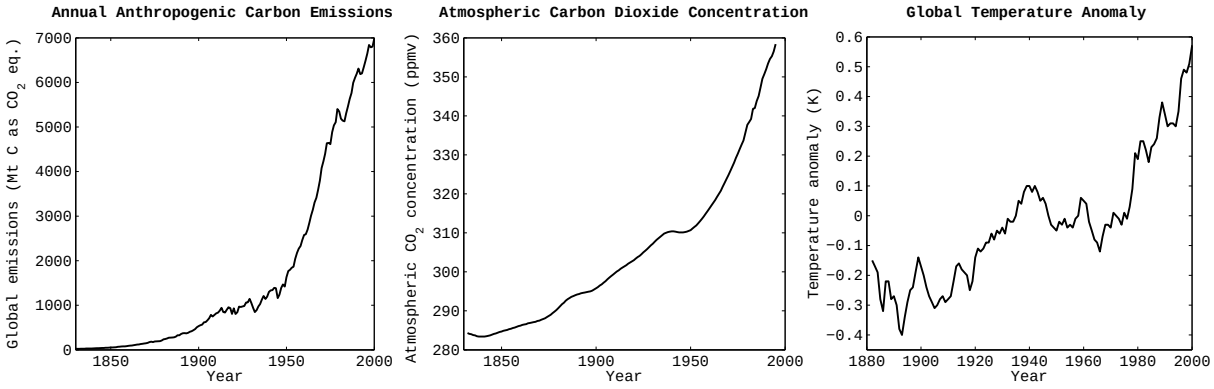

Figure 1: Carbon and temperature trends (Raw data: CDIAC).

The current and expected effects of global warming are well documented, although there is disagreement on their expected severity. The earliest predictions of the warming effects of atmospheric CO_2 were made in the 19th century.[3] Recent studies predict an increase in phenomena such as extreme weather events, glacier and sea ice retreat, sea level rise, ocean acidification, the shutdown of oceanic thermohaline currents, forest fires, and changes to the carbon and water cycles. These geophysical effects in turn are likely to lead to widespread economic and political upheaval, exacerbated by resource shortages. Other effects include wholesale species extinction and the spread of disease.

[1] Some exceptions remain, as publicised recently in a controversial TV documentary [1].

[2] Similar graphs exist for other greenhouse gases such as methane, but it is common to bundle these figures together into an "equivalent CO_2" measure, since the climatic effects of the gases are qualitatively similar.

[3] The first *quantitative* prediction was made by Arrhenius in 1896: a 5 to 6 °C rise for a doubling of atmospheric CO_2. The history of GHG theory is discussed in chapter 2 of Houghton's book [11].

There are two options for mitigating these effects. The first option, and the currently accepted one, is to attempt to reduce GHG emissions sharply (by 50-80%) over the next few decades, through energy efficiency and low-carbon generation. However, aside from the strong political will power required, this approach has inherent problems in that temperature changes are a function of current greenhouse gas concentrations, and not current emission rates, i.e. there is a lag of the order of 50-100 years before the effects of any reduction can be enjoyed. The second option is to fund one or more global engineering schemes (often termed "geo-engineering") to control the climate actively. Several figures, the most famously controversial being Edward Teller, have argued [16, 21, 38] that there is little hope of preventing a crisis by gradual political means, and that mankind should invest in a climate "Manhattan Project" [21] soon in order to avert disaster. Some possible schemes and their likely effects are discussed in §5.1.

1.2 Motivation

Much research has been carried out in the last few decades on modelling the effects of mankind's activities on the earth's climate, and sophisticated three-dimensional computer models (General Circulation Models, or GCMs) have been developed for this purpose. Many of these simulations attempt to involve a large number of the different mechanisms that have been found to affect the climate, with increasingly fine spatial and temporal resolution. However, because of the uncertainties inherent in measuring and reproducing many of these factors, the accuracy of their forecasts is in many cases questionable given the human and computational investment made. This is the primary reason for the wide range of (often conflicting) climate change predictions reported by the media.

Clearly the development of such a model would be outside the scope of this project, and its relevance to engineering science tenuous. The approach here is to develop a simple one-dimensional simulation that still models the main climate mechanisms, and then to use control theory to make judgments on the effects of human intervention in climate change scenarios. The main challenges when attempting this are to produce globally-averaged expressions for complex, globally-varying phenomena, and to reduce the number of dependencies by identifying the most significant inputs. For example, the infrared emissions of the upper atmosphere to space depend on water vapour content, local temperature, vapour distribution and the concentration of many different absorbing atmospheric compounds, but we may want to reduce this to a global average function of only one or two variables, but which has roughly the same sensitivity to variation of its inputs.

1.3 Classification of Climate Models

There exists a wide range of climate models, developed in order to draw different kinds of conclusion on future climate change. When choosing such a modelling scheme, the most common trade-off, as phrased by the IPCC report [12], is comprehensiveness versus complexity.

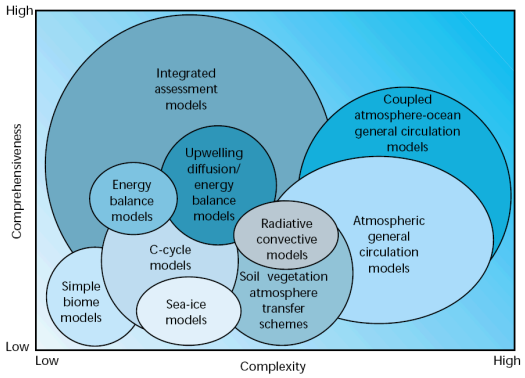

Figure 2: Classification of climate models (Source: IPCC)

For a given effort spent in development, a model may simulate a specific effect (for example, the melting of polar ice) with a high degree of accuracy, or make broader generalisations about a wide range of effects with much less accuracy, typically by averaging distributed variables (for example, local surface sea temperature) as a single parameter. Fig. 2 illustrates some of the common classifications of model in use. These models represent a trade-off between the following factors:

- Computational complexity. Three-dimensional circulation models are orders of magnitude more computationally expensive than simple box models, since it is necessary to solve PDEs governing diffusion and mass flow in the oceans and atmosphere.
- The time required to collate geophysical data (such as annual temperature variation by location), and the availability of such data.
- The degree of information loss through averaging. For example, the ocean's temperature might be parameterised as three depth zones whose temperatures are weighted averages over the global distributions.
- The comprehensiveness of the model. For example, a model paying particular attention to ocean current feedbacks may be poor at simulating atmospheric effects.

1.4 Project Objectives

1. To use authoritative literature (for example as referenced by IPCC Technical Paper II [12]) as a guide to developing a box model of the earth's main climate mechanisms:

   (a) Determine an appropriate set of reservoirs that consitutes an appropriate trade-off between realism and simplicity.

   (b) Derive simplified relationships between the rates of heat and carbon transfer between reservoirs and the states of those reservoirs, based on parameterisations found in literature.

2. To convert the above into a state-space model, to which familiar control theory concepts can be applied.

   (a) Linearise this model and compare with the non-linear model.

3. To ensure the model developed exhibits similar forcing responses to comparable efforts in literature.

4. To forecast the effects of different greenhouse gas emissions scenarios.

5. To model the effects of implementing active climate control (ACC) solutions:

   (a) Discuss recently-suggested geo-engineering countermeasures to the global warming problem.

   (b) Describe the implementation of a few of these methods from a control systems perspective, including as an optimisation problem.

   (c) Draw conclusions on the viability of these schemes.

2 Model Development

Of the time spent developing the model described below, a significant proportion has been allocated to reviewing literature. The IPCC report provides a useful summary of important work using simple climate models (SCMs), and in particular points to Harvey and Schneider [9] as a good starting point. In addition, Harvey's book [7] has provided much of the background information necessary for a qualitative understanding of the climate system.

Harvey and Schneider has formed the starting point for the thermal components of the model (§2.2), although there have been some challenges in achieving similar results (see §9). Parallel to the thermal cycle, a carbon cycle based on a range of literature was developed (§2.3), and finally functional relationships were collected in order to proved the feedbacks between the cycles (§2.4).

2.1 Model Outline

The box model consists of coupled thermal and carbon cycles. In each cycle, transfers representing the most significant climate processes take place between the different reservoirs ("boxes"), the rates of which are solely dependent on the states of the reservoirs. The rates of heat transfer in the thermal cycle may also be functions of the carbon reservoir conditions, and vice versa.

The model is outlined in Fig. 3. The symbols are explained in Table 1. The model has been implemented in *MATLAB*.

	Thermal Cycle		**Carbon Cycle**
$Q_A^\star$	SWR absorbed in the atmosphere	F	Fossil fuel combustion
$Q_S^\star$	SWR absorbed at the surface	P	Photosynthesis
L_{OUT}	IR emitted to space	R	Reforestation
$L_\uparrow$	IR transfer from surface to atmosphere	D	Deforestation
$L_\downarrow$	IR transfer from atmosphere to surface	C	Oceanic carbon diffusion
H	Latent heat flux	V	River flux
LE	Turbulent heat flux	U	Biological pump
$S_{X\to Y}$	Thermohaline current heat transfers	I	Diffusion between ocean layers
$M_{S\to I}$	Mixing between surface and int. layers	B	Bulk convection transport
		E	Sedimentation

Table 1: Terms used in Fig. 3.

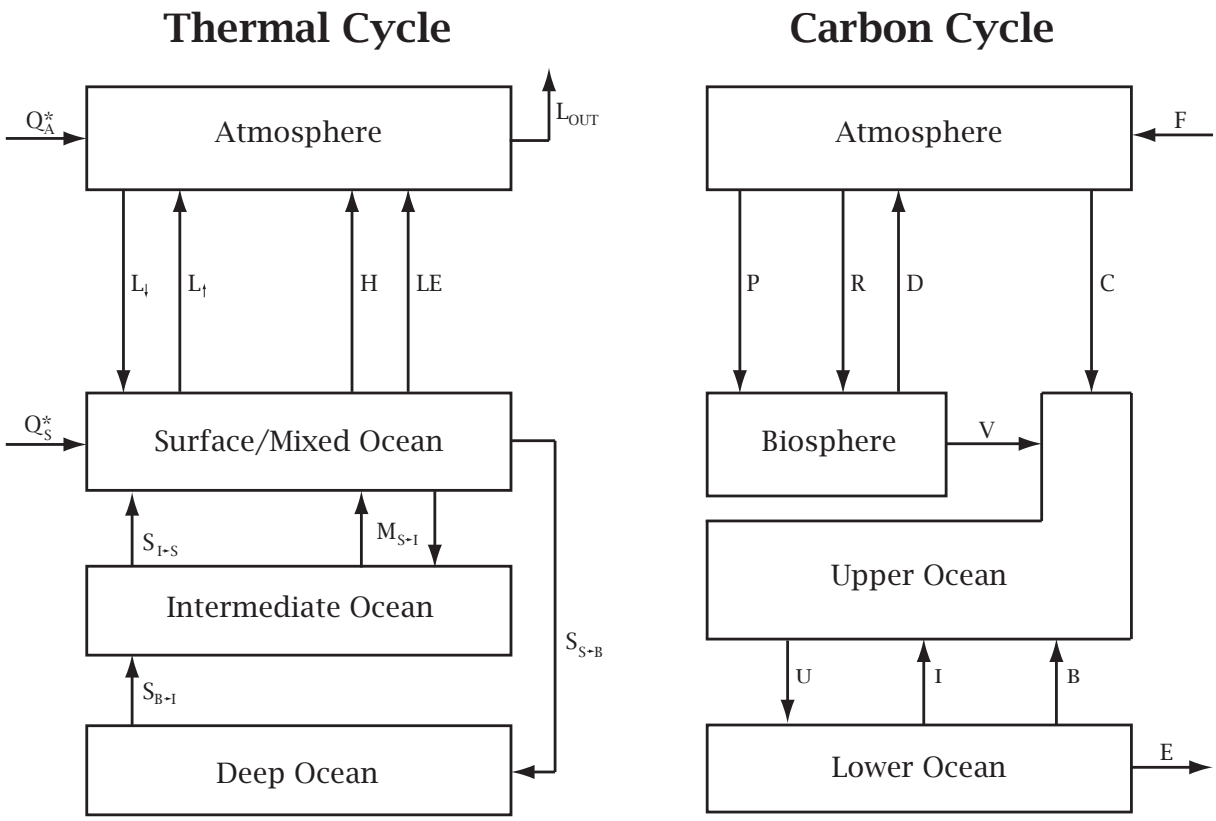

Figure 3: Model Outline

2.1.1 Thermal Cycle

The thermal cycle comprises four isothermal heat reservoirs, modelling respectively the atmosphere, surface ocean layer, intermediate ocean layer and bottom ocean layer. Each reservoir represents a globally-averaged quantity and obeys the following energy conservation law *for a square metre of land area:*

$$R\frac{\mathrm{d}T}{\mathrm{d}t} = \sum P_{in}^{T}(\mathbf{T},\mathbf{C}) - \sum P_{out}^{T}(\mathbf{T},\mathbf{C}) \tag{1}$$

where R is the reservoir's thermal capacity in J K^{-1}, T is its temperature in K, time t is measured in years, P_{in}^{T} and P_{out}^{T} are per-square-metre rates of heat transfer into and out of the reservoir. These rates are assumed to be time-invariant and are functions only of the vectors of reservoir temperatures $\mathbf{T}$ and/or carbon quantities $\mathbf{C}$.[4]

2.1.2 Carbon Cycle

The carbon cycle comprises four separate carbon reservoirs, modelling respectively the atmosphere, terrestrial biosphere (sum of living and dead organic biomass on the land

[4]The time-invariance assumption is discussed further in §2.5.

surface), surface ocean layer and bottom ocean layer. *Note that the carbon reservoirs are not intended to coincide physically with the thermal reservoirs.* Each reservoir obeys the following conservation law:

$$\frac{\mathrm{d}C}{\mathrm{d}t} = \sum P_{in}^{C}(\mathbf{T}, \mathbf{C}) - \sum P_{out}^{C}(\mathbf{T}, \mathbf{C}) \tag{2}$$

where C is the quantity of carbon in the reservoir in gigatons of carbon *equivalent* (Gt C),[5] P_{in}^{C} and P_{out}^{C} are carbon transfer rates into and out of the reservoir. Again, the carbon transfer rates R are time-invariant and are again functions only of reservoir temperatures and/or carbon quantities.

2.2 Modelling the Thermal Cycle

2.2.1 Choice of Reservoirs

Given the choice of the modelling scheme described in subsection 2.1, it is necessary to decide which components of the climate to represent. The ocean layers, land surface and atmospheric layers all influence heat transfers associated with climate change processes. Fortunately, as shown by Harvey and Schneider [9], it is possible to pare these physical entities down to just a handful of variables while keeping a grip on the physical processes of interest; these processes are described in the following section. The reservoirs chosen are those chosen by Harvey and Schneider, and are defined per square metre of land area:

1. **Atmosphere:** Represents the thermal inertia of all particles occupying the space above a square metre of land area.
2. **Land Surface/Mixed Sea Layer:** Represents a weighted average of the land's surface thermal inertia[6] and top 30 metres of the ocean.[7]
3. **Intermediate Sea Layer:** Seawater at depths between 30 m and 1500 m.
4. **Bottom Sea Layer:** All seawater deeper than 1500 m.

[5] This is the sum of the masses of the carbon components of all compounds present in the reservoir. In the atmosphere, carbon is largely present as CO_2 and CH_4. 1Gt C is equivalent to 3.7 Gt CO_2. In the oceans, carbon is mostly found in Dissolved Inorganic Carbon (DIC) compounds, as $[CO_3]^{2-}$ and $[HCO_3]^{-}$ ions.

[6] Only the top few metres of the land mass change temperature appreciably throughout the course of a year, so the thermal mass below this depth is not considered part of the model.

[7] This region is known as the "mixed sea layer" because mixing caused by surface turbulence results in temperatures roughly constant across the depth of the layer.

The four reservoirs have absolute temperatures T_A, T_S, T_I, and T_B respectively, and their heat capacities are R_A, R_S, R_I, and R_B.

2.2.2 Heat Transfer Processes

The heat transfers that take place on earth that could potentially be incorporated into the model are numerous and complex. They include:

- Absorption, transmission and reflection of incoming solar energy
- Black-body (infrared) radiation emitted from the earth's surface and atmosphere
- Embodied energy in water transfers (precipitation, evaporation etc.)
- The thermohaline circulation in the oceans driven by the sinking of cold polar water
- Bulk mixing between the surface and sea layers

Clearly these effects vary with latitude (for example, the reflection of direct sunlight from polar ice), and season (for example, cloud cover over a particular location varies during the course of a year). Moreover, some significant effects are specific to peculiarities in the arrangement of the continents (for example, the Gulf Stream).

In order to fulfil our desire to make a meaningful control-systems assessment, we need to distill these processes down to simple functions of the state variables chosen for the system. It is therefore apparent that data for these processes need to be collected and averaged, annually and over the surface of the earth, weighting according to insolation and area where necessary. Much of this effort was collated by Harvey and Schneider, and the parameterisations are summarised in the following paragraphs.

***Shortwave Radiation:* $Q^\star_A$ *and* $Q^\star_S$**

Many attempts to parameterise the absorption of SWR in the atmosphere (such as [14]), but most are too complicated for this project. The SWR scheme here is adapted from a paper by Thompson and Barron [37]. The rates of shortwave solar energy absorption by the atmosphere and surface, $Q^\star_A$ and $Q^\star_S$ respectively, depend on the geographical location (here we assume only variation with latitude θ due to the averaging effect of the earth's rotation), time of year (due to the change in the earth's tilt), and the mean temperature of the earth. In order to obtain a globally averaged per-square-metre

value for these two variables, it is necessary to take an area- and insolation-weighted average of the distribution found across the earth. Given a latitude θ and a global mean temperature T_{mean}, the weighted average is given by

$$Q_A^\star(T_{mean}) = \frac{\int_{-\pi/2}^{+\pi/2} Q_{total}(\theta) Q_A^\star(\theta, T_{mean}).2\pi R.R\cos\theta \ \mathrm{d}\theta}{\int_{-\pi/2}^{+\pi/2} Q_{total}(\theta).2\pi R.R\cos\theta \ \mathrm{d}\theta} \tag{3}$$

$$Q_S^\star(T_{mean}) = \frac{\int_{-\pi/2}^{+\pi/2} Q_{total}(\theta) Q_S^\star(\theta, T_{mean}).2\pi R.R\cos\theta \ \mathrm{d}\theta}{\int_{-\pi/2}^{+\pi/2} Q_{total}(\theta).2\pi R.R\cos\theta \ \mathrm{d}\theta} \tag{4}$$

where R is the mean radius of the earth (a spherical approximation is made here), Q_{total} is the intensity of incoming solar radiation, $Q^\star$ is the absorbed radiation intensity, and $2\pi R.R\cos\theta\delta\theta$ is the approximate area of an elemental strip on the earth's surface lying in the interval $[\theta,\ \theta+\delta\theta]$.

As an approximation, the continuous latitude θ is replaced by 17 discrete latitude bands i of width 10° centred on θ_i, so that equations (3) and (4) become

$$Q_A^*(T_{mean}) = \frac{\sum_{i=1}^{17} Q_i^{total} Q_{A,i}^\star(T_{mean}) A_i}{\sum_{i=1}^{17} Q_i^{total} A_i} \tag{5}$$

$$Q_S^*(T_{mean}) = \frac{\sum_{i=1}^{17} Q_i^{total} Q_{S,i}^\star(T_{mean}) A_i}{\sum_{i=1}^{17} Q_i^{total} A_i} \tag{6}$$

where band i has area $A_i = \int_{\theta_i-5^\circ}^{\theta_i+5^\circ} 2\pi R^2\cos\theta d\theta$, and receives solar energy at average intensity Q_i^{total}. This is so that the data presented by Thompson and Barron [37] (see Table 5) can be used to compute the average. To fit this model, the absorptions could not be calculated in the same way as in [37], therefore an adapted scheme was developed to to calculate each $Q_{A,i}^\star$ and $Q_{S,i}^\star$: see the appendix §9.

Infrared Radiation: $L_\uparrow$***,*** $L_\downarrow$ ***and*** L_{OUT}

For a surface with temperature distribution T and an emissivity ("blackness") distribution $0 \le \varepsilon \le 1$, the rate of thermal radiation W is given by the Stefan-Boltzmann Law $W = \sigma \int \varepsilon T^4 dA$, where $\sigma = 5.6704 \times 10^{-8}$ is the Stefan-Boltzmann constant.

In the case of the earth, thermal radiation is emitted from the surface and also throughout the atmosphere. At earth temperatures virtually none of the emission spectrum falls in the visible (shortwave) range,[8] so it is appropriate here to use the term "infrared radiation" interchangeably with "black-body radiation."

For this model, the simplification adopted from Harvey and Schneider has been to parameterise the processes as follows:

- Surface IR energy transferred to the atmosphere

$$L_{\uparrow} = \sigma T_S^4 \tag{7}$$

- Atmospheric IR energy transferred to the surface

$$L_{\downarrow} = \varepsilon_{\downarrow} \sigma T_A^4 \tag{8}$$

  with $\varepsilon_{\downarrow} = 0.89 - 0.2 \times 10^{-0.07 e_A}$, where e_A is the saturation vapour pressure.

- Atmospheric IR emissions to space

$$L_{OUT} = A + BT_A - CF_{CL}\Delta T_{S,CL} \tag{9}$$

  where constants $A = -251\,\mathrm{W}$, $B = 1.8\,\mathrm{W\,K^{-1}}$, and $C = 1.73\,\mathrm{W\,K^{-1}}$, $F_{CL} = 0.544$ is the globally-averaged cloud fraction and $\Delta T_{S,CL} = 32.34\,\mathrm{K}$ is the mean temperature difference between the earth's surface and the top of the cloud layer.[9]

Sensible and Latent Heat Fluxes: H ***and*** LE

Heat transfers at the boundary between the earth's surface and the atmosphere happen in two ways, and the following simplifications are made with reference to Harvey and Schneider. Further information on the nature of these processes is given in [28]. Sensible heat flux H (heat flux due to conduction and subsequent convection currents caused by the temperature difference between the surface and atmosphere) is defined by

$$H = C_1(T_S - T_A) \tag{10}$$

[8] Wien's Law predicts a radiation spectrum peak at wavelength $\lambda_{max} = \frac{b}{T}$, where b is a constant equal to 2.90×10^{-3} m K. Earth surface temperatures averaging about 288 K give a peak wavelength of around 10^{-5} m, well into the infrared range.

[9] This parameterisation is from Ramanathan [24].

where C_1 is a constant equal to 12.57 W m^{-2} K^{-1}. Latent heat flux LE (heat flux embodied in evaporation of water from the sea and land surfaces) is defined by

$$LE = C_2(e_S - e_A) \tag{11}$$

where e_S and e_A are the saturation vapour pressures (in mbar) at temperatures T_S and T_A,[10] and C_2 is a constant equal to 11.75 W m^{-2} mbar^{-1}.

Thermohaline current: $S_{S\to B}$, $S_{B\to I}$, $S_{I\to S}$

Surface seawater at the poles is known to cool and sink due to the relative increase in its density and changes in salinity. This process forms part of a current whereby water resurfaces again nearer the equator. Fig. 11.2 of Harvey's book [7] illustrates this process. Heat transfers are embodied in this current, represented here by the parameters $S_{S\to B}$, $S_{B\to I}$, and $S_{I\to S}$. The per-square metre rates are given by the equations:

$$S_{S\to B} = \frac{\dot{V}}{\sigma_G} c_w (T_S - T_B) \quad \text{(Surface to bottom layer)} \tag{12}$$

$$S_{B\to I} = \frac{\dot{V}}{\sigma_G} c_w (T_B - T_I) \quad \text{(Bottom to intermediate layer)} \tag{13}$$

$$S_{I\to S} = \frac{\dot{V}}{\sigma_G} c_w (T_S - T_B) \quad \text{(Intermediate to surface layer)} \tag{14}$$

where $\dot{V} = 1.527 \times 10^{15}$ m^3 yr^{-1} is the thermohaline mass flux (derived from empirical measurements), $\sigma_G = 5.101 \times 10^{14}$ m^2 is the global surface area, and $c_w = 4181$ kJ kg^{-1} K^{-1} is the specific heat capacity of water.

Mixing between the surface and intermediate layers: $M_{S\to I}$

In addition to the bulk transfer under the action of the thermohaline current, turbulent mixing takes place between the surface and intermediate sea layers. The embodied energy in this transfer $M_{S\to I}$ is given by

$$M_{S\to I} = \frac{V_S}{\tau_{S\to I}\sigma_G} c_w (T_S - T_I) \text{ Transfer from surface to intermediate sea layer} \tag{15}$$

where $V_S = 30 \times 0.708 \times \sigma_G = 1.083 \times 10^{15}$ m^3 is the total volume of the surface layer of the earth's oceans, and $\tau_{S\to I} \approx 10$ yr is the turnover time, based on the detailed model of Sarmiento et al. [31].

[10] This is calculated using a polynomial fit calculated by Lowe [18]. In fact, to allow for the non-linearity of the Clausius-Clapeyron relation (which governs the saturation limit of water in air) when taking weighted averages, e_A and e_S are multiplied by 1.31 and 1.39 respectively before use in these global formulae [9].

2.3 Modelling the Carbon Cycle

2.3.1 Choice of Reservoirs

As with the thermal reservoirs, it would be possible to include virtually any number of carbon reservoirs in the model, with the quantities of carbon in each having their own effects on climate feedbacks. However, many important carbon transfer processes are quite poorly understood; chapter 8 of Harvey's book [7] gives an overview of the often conflicting results of research efforts into carbon cycle components.

In light of this, it is better to err on the side of simplicity: four reservoirs are chosen here, representing a simplification of a model used for a recent publication from the Royal Society on ocean acidification [27]. Note that unlike the thermal reservoirs, these reservoirs represent whole earth quantities rather than per-square-metre quantities:

1. **Atmosphere:** The carbon contained in compounds in the earth's atmosphere.
2. **Terrestrial Biosphere:** The sum of carbon embodied in all living and dead organic matter on the land
3. **Upper Sea Layer:** Carbon present in all compounds and organic material present down to a depth 100 metres.
4. **Lower Sea Layer:** Carbon present in all compounds at depths greater than 100 metres.

The quantities of carbon (in equivalent Gt C) present in the reservoirs are denoted C_1, C_2, C_3, and C_4 respectively.

2.3.2 Carbon Transfer Processes

The heat transfers described in §2.2.2 operate according to well-understood physical laws. In contrast, it is much harder to measure or form hypotheses regarding the processes which govern the carbon cycle. Nevertheless, it is generally agreed tha the processes described here play the most significant parts in the carbon cycle.

Net Photosynthesis and Respiration: P

Numerous studies (such as [6, 13]) have attempted to find a relationship between the growth rate of plants, i.e. the rate of photosynthesis, and the levels of CO_2 in the air

surrounding them. Although many other environmental factors (particularly scarcity of other resources) influence the relationship, the broad consensus from these, as discussed by Harvey, is that although an initial increase in CO_2 enrichment brings about substantial gains in the rate of photosynthesis, further increases offer diminishing returns. Fig. 8.1 of Harvey's book [7] gives some results from controlled experiments of this kind.

Plants are built from conversion of atmospheric CO_2 into glucose by photosynthesis. At the same time, cellular respiration releases some of this trapped carbon. These two processes can be seen in simplified form as changes in direction of the reaction

$$6\ CO_{2(g)} + 12\ H_2O_{(l)} \rightleftharpoons C_6H_{12}O_{6(aq)} + 6\ O_{2(g)} + 6\ H_2O_{(l)}$$

with the left-to-right (photosynthetic) reaction requiring input of solar energy. In general, a given plant will be a net photosynthesiser by day and a net respirer by night; over longer timescales it can be assumed that no net transfer takes place unless the plant is growing or dying. We therefore expect that if the rate of reaction is limited by CO_2 levels in the air, then an increase in atmospheric CO_2 concentration will increase the rate of photosynthesis and cause new plant growth. In terms of the reservoirs defined above, an increase in C_1 will cause an increase in the rate of carbon transfer from carbon reservoir 1 to carbon reservoir 2. The discussion of how these principles extend to a law for the whole-earth biosphere is involved and beyond the scope of this report (see [7]), but based on Harvey's arguments the following law for P was chosen based on a scaled curve fit for Harvey's data:

$$P = 0.5 + 0.85k \times (1 - e^{\frac{C_1 - C_{10}}{1000}}) \tag{16}$$

where $k = 1$ Gt yr^{-1} is a scaling factor and C_{10} is the initial equilibrium value of C_1. Note that the offset of 0.5 Gt yr^{-1} is balanced by river flux V (see below), which represents the transport of organic carbon by river transport into the sea. Historically this equilibrium has never actually existed, but it is necessary to include the offset to allow an equilibrium, and the offset will disappear once we take a linearisation later.

Net carbon transfer to oceans: C

The oceans' vast contact area with the atmosphere plays a very important role in the carbon cycle. As the level of carbon dioxide in the atmosphere increases, a carbon transfer takes place as the concentration of the gas dissolved in the upper ocean layers increases in response. This rate of transfer is proportional to the difference in partial pressures of CO_2:

$$C = k_{as}(\mathrm{p}[CO_2]_{atm} - \mathrm{p}[CO_2]_{ocean}) \tag{17}$$

where $k_{as} = 1.119$ Gt C yr$^{-1}\mu$atm^{-1}. The partial pressures (measured in μatm) are governed by

$$\begin{aligned} \text{p}[\text{CO}_2]_{atm} &= 0.469 C_1 \\ \text{p}[\text{CO}_2]_{ocean} &= \frac{\text{Conc}[\text{CO}_2]_{ocean}}{\alpha_{\text{CO}_2}(T_2)} \\ \text{where} \quad \text{Conc}[\text{CO}_2]_{ocean} &= 9.08 \times \frac{C_3}{C_{30}} \end{aligned}$$

where $\alpha_{\text{CO}_2}(T_2)$ is the solubility of CO_2 in water[11] and $\text{Conc}[\text{CO}_2]_{ocean}$ is the concentration of CO_2 in the upper sea layer in μmol l^{-1}.

River Flux: V

The transfer of organic material from the terrestrial biosphere to the sea is poorly understood. Harvey [7] estimates that the current rate of transfer due to this effect as about 0.5 Gt yr^{-1}. Here a simple proportionality with the amount of biomass present is assumed:

$$V = 0.5 \frac{C_2}{C_{20}} \tag{18}$$

Fossil Fuel Burning: F

As fossil fuels are burned, CO_2 is released to the atmosphere. The rate F is considered to be an input to our system. Scenarios for future CO_2 emissions of this type are discussed in §4.2.1.

The Biological Pump: U

The "biological pump" is a term used to describe the effect of organisms growing, accreting carbon in forms such as carbonate shells, and then dying and sinking to the ocean floor. The net effect of this process is a current of carbon from the upper ocean to the deep ocean. This process is sustained by the solar energy input that allows the plant life such as algae, on which all sea life depends, to grow. Here we assume a constant rate, since the pump is limited by factors such as nutrient supply, which are not modelled:[12]

$$U = 10.38 \text{ Gt yr}^{-1} \tag{19}$$

[11] Although the mixed sea layer thermal reservoir does not exactly coincide with the upper sea carbon reservoir defined in this section, its temperature is used as an approximation. The poynomial fit $\alpha_{\text{CO}_2}(T_2) = 8.8031218 - 0.0814192\,T_2 + 2.5257 \times 10^{-4}\,T_2^2 - 2.6233 \times 10^{-7}\,T_2^3$ is used here.

[12] The steady-state values of the quantities defined here as U, I and E are taken from table 8.3 of Harvey's book [7].

Oceanic Carbon Diffusion: I

At the boundary between the deep sea, which is highly concentrated with DIC, and the surface, diffusion of carbon compounds takes place. This rate is assumed to be proportional to the concentration difference between the layers, with a baseline rate of 7.97 Gt yr^{-1}:

$$I = 7.97 \times \frac{\left(\frac{C_4}{V_4} - \frac{C_3}{V_3}\right)}{\left(\frac{C_{40}}{V_4} - \frac{C_{30}}{V_3}\right)} \tag{20}$$

Oceanic Bulk Carbon Transfer: B

Convection and advection in the oceans produce a net transfer of carbon to the surface layer by replacing surface water with more highly concentrated deep-sea water. The (constant) rate for this is taken as:

$$B = 2.41 \text{ Gt yr}^{-1} \tag{21}$$

Deep-ocean Sedimentation: E

Sedimentation of solid carbon compounds onto the ocean beds plays an important role in climate regulation; a strategy for climate change mitigation proposed recently by James Lovelock [17] and quickly seized upon by the press [5, 20] involves encouraging an increase in the rate of the biological pump such that the rate of sedimentation, and eventually carbon sequestration from the atmosphere, would increase. Here the rate of sedimentation (a transfer of carbon out of the model boundaries) is proportional to the excess carbon present in the bottom ocean layer; the initial condition $C_4 = C_{40}$ is assumed to represent a lower ocean layer saturated with DIC.

$$E = k_{sed}\frac{C_4 - C_{40}}{C_{40}} \tag{22}$$

where $k_{sed} = 1$ Gt yr^{-1} is a constant of proportionality based on the rate of precipitation of solids out of a saturated solution.

2.4 Coupling the Thermal and Carbon Cycles

2.4.1 The Greenhouse Effect

One of the major feedbacks responsible for warming of the atmosphere is *radiative forcing* due to increased carbon concentration in the atmosphere, known as the Greenhouse

Effect. An increase in atmospheric CO_2 causes a change in the balance between infrared emissions from the atmosphere back to earth and emissions from the atmosphere out to space, so that the net thermal energy retained in the system is increased. Consequently, temperatures increase until infrared emissions are in equilibrium with the higher proportion of retained solar radiation, at which point a higher steady-state temperature distribution is reached. Here the radiative forcing law is taken from a parameterisation taken from §6.3 of the IPCC report [25]:

$$\Delta L_{\downarrow} = -\Delta L_{OUT} = 5.41 \ln(C_1/C_{10}) \tag{23}$$

so that, from (8) and (9), we obtain:

$$L_{\downarrow} = \varepsilon_{\downarrow}\sigma T_A^4 + 5.41 \ln(C_1/C_{10}) \tag{24}$$

$$\text{and} \quad L_{OUT} = A + BT_A - CF_{CL}\Delta T_{S,CL} - 5.41 \ln(C_1/C_{10}) \tag{25}$$

2.4.2 The Effect of Global Warming on the Thermohaline Current

Studies have suggested that, via the increased DIC in surface seawater, excess atmospheric CO_2 causes a reduction in the flux rate of the THC. Harvey [7] cites several examples of how this effect may be modelled, coming to the conclusion that a 40% reduction for a doubling of atmospheric CO_2 is a sensible approximation. Hence, from (12), (13) and (14), we obtain:

$$S_{S\to B} = \frac{\dot{V}}{\sigma_G} c_w (T_S - T_B) \left(1 - 0.4 \times \frac{C_1 - C_{10}}{C_{10}}\right) \tag{26}$$

$$S_{B\to I} = \frac{\dot{V}}{\sigma_G} c_w (T_B - T_I) \left(1 - 0.4 \times \frac{C_1 - C_{10}}{C_{10}}\right) \tag{27}$$

$$S_{I\to S} = \frac{\dot{V}}{\sigma_G} c_w (T_S - T_B) \left(1 - 0.4 \times \frac{C_1 - C_{10}}{C_{10}}\right) \tag{28}$$

2.5 Time Invariance

From the above descriptions it is clear that we are not incorporating:

a) any time lags in feedbacks (for example a relationship of the form $\dot{\mathbf{x}} = \mathbf{g}(\mathbf{x}(t-\tau))$), and

b) any other long-term changes in factors which may affect heat or carbon transfer rates, such as geological activity.

Where a lag approximation may have been useful (one example is when modelling carbon dioxide diffusion between the atmosphere and oceans), the lag in question was less than 10 years. Given that we are interested in much longer time scales than this, though, it was judged safe to assume that neglecting them will not alter our conclusions. In addition, lags would be difficult to implement while keeping the control analysis simple.

2.6 Model Limitations

As can be expected from a vastly simplified model, there are limits as to what the scheme described above can predict. The most obvious result of global averaging is the lack of any capability to make predictions on local effects, for example local heating extremes or changes to the distribution of forests. Box model limitations are discussed further in [23]. However, [9] showed that a box model of the ocean could yield similar results to a simple PDE-based diffusion model, which suggests we are on the right side of the simplicity trade-off for studying the earth as a control system.

This report also focuses on concepts of stability and equilibrium which historically have never applied to the earth's climate system. Firstly, the box model for the thermal cycle only reaches equilibrium when all sea layers are at the same temperatures; in the real system this is not the case because of heat flow to the sea bed, which is outside our model boundary. Secondly, the earth's carbon cycle has never been in an equilibrium, since river flux has never felt a need to converge to the rate at which photosynthesis adds to terrestrial biomass.

3 The Climate as a Control System

3.1 State Space Realisation

The key objective of the project is to analyse the climate system by reduction to familiar control system theory. With this in mind, the relationships described above are most succinctly reduced to a state-space form, the expansion of which is shown in Fig. 4:

$$R\dot{\mathbf{x}} = G\mathbf{f}(\mathbf{x}) + H\mathbf{u} \tag{29}$$

where

- R is an $n \times n$ diagonal matrix, scaling the upper rows corresponding to the heat capacities of the four thermal reservoirs while leaving the lower rows unscaled;
- $\mathbf{x} = [x_1 \quad x_2 \quad \dots \quad x_8]^T =: [T_A \ T_S \ T_I \ T_B \ C_1 \ C_2 \ C_3 \ C_4]^T$ is the state vector of dimension $n = 8$, with four states representing the absolute temperatures of the four reservoirs from §2.2.1 and four states representing the quantities of carbon present in the four reservoirs from §2.3.1;
- G is an $n \times q$ matrix with entries equal to 0, +1 or -1, specifying the sources and destinations of the heat and carbon transfers ($g_{ji} = -1$; $g_{ki} = +1$ indicates a transfer f_i from reservoir j to reservoir k);
- $\mathbf{f}$ is a q-element column vector specifying the magnitudes of the heat and carbon transfer processes as functions of the current state (there are $q = 18$ processes);
- H is a $n \times m$ matrix with entries equal to 0, +1 or -1, specifying the sources and destinations of the heat and carbon transfers considered to be inputs, in the same way as matrix A;
- $\mathbf{u}$ is an m-element column vector, specifying the magnitudes of the m input processes.

R is inverted[13] for the more standard form

$$\dot{\mathbf{x}} = R^{-1}G\mathbf{f}(\mathbf{x}) + R^{-1}H\mathbf{u} \tag{30}$$

3.2 Linearisation

The system described by (30) can be linearised to the form

$$\dot{\boldsymbol{\delta}\mathbf{x}} = R^{-1}GF\boldsymbol{\delta}\mathbf{x} + R^{-1}H\boldsymbol{\delta}\mathbf{x} \tag{31}$$

where $\boldsymbol{\delta}\mathbf{x} = \mathbf{x} - \mathbf{x}_0$ and F is a $q \times n$ matrix given by

$$F = \frac{\partial \mathbf{f}}{\partial \mathbf{x}} = \begin{bmatrix} \frac{\partial f_1}{\partial x_1} & \dots & \frac{\partial f_1}{\partial x_n} \\ \vdots & \ddots & \vdots \\ \frac{\partial f_q}{\partial x_1} & \dots & \frac{\partial f_q}{\partial x_n} \end{bmatrix}$$

[13] Since R is diagonal, its inversion is given simply by $[R^{-1}]_{ij} = \frac{1}{\{r_{ij}\}}$ for $i = j$, 0 otherwise.

$$
\begin{bmatrix}
R_A & 0 & 0 & 0 & 0 & 0 & 0 & 0 \\
0 & R_S & 0 & 0 & 0 & 0 & 0 & 0 \\
0 & 0 & R_I & 0 & 0 & 0 & 0 & 0 \\
0 & 0 & 0 & R_B & 0 & 0 & 0 & 0 \\
0 & 0 & 0 & 0 & 1 & 0 & 0 & 0 \\
0 & 0 & 0 & 0 & 0 & 1 & 0 & 0 \\
0 & 0 & 0 & 0 & 0 & 0 & 1 & 0 \\
0 & 0 & 0 & 0 & 0 & 0 & 0 & 1
\end{bmatrix}
\begin{bmatrix} \dot{x}_1 \\ \dot{x}_2 \\ \dot{x}_3 \\ \dot{x}_4 \\ \dot{x}_5 \\ \dot{x}_6 \\ \dot{x}_7 \\ \dot{x}_8 \end{bmatrix}
=
\begin{bmatrix}
+1 & 0 & -1 & +1 & +1 & +1 & +1 & 0 & 0 & 0 & 0 & 0 & 0 & 0 & 0 & 0 \\
0 & +1 & 0 & -1 & -1 & -1 & -1 & 0 & +1 & -1 & +1 & 0 & 0 & 0 & 0 & 0 \\
0 & 0 & 0 & 0 & 0 & 0 & 0 & +1 & -1 & 0 & 0 & 0 & 0 & 0 & 0 & 0 \\
0 & 0 & 0 & 0 & 0 & 0 & 0 & +1 & -1 & 0 & 0 & 0 & 0 & 0 & 0 & 0 \\
0 & 0 & 0 & 0 & 0 & 0 & 0 & 0 & 0 & 0 & -1 & 0 & 0 & 0 & 0 & 0 \\
0 & 0 & 0 & 0 & 0 & 0 & 0 & 0 & 0 & 0 & +1 & -1 & 0 & 0 & 0 & 0 \\
0 & 0 & 0 & 0 & 0 & 0 & 0 & 0 & 0 & 0 & 0 & +1 & +1 & -1 & +1 & +1 \\
0 & 0 & 0 & 0 & 0 & 0 & 0 & 0 & 0 & 0 & 0 & 0 & 0 & +1 & -1 & -1
\end{bmatrix}
\begin{bmatrix}
Q_A^\star(x_1) \\
Q_S^\star(x_1) \\
L_\uparrow(x_2) \\
L_\downarrow(x_1, x_5) \\
L_{OUT}(x_1, x_5) \\
H(x_1, x_2) \\
LE(x_1, x_2) \\
S_{S\to B}(x_2, x_4, x_5) \\
S_{B\to I}(x_3, x_4, x_5) \\
S_{I\to B}(x_2, x_3, x_5) \\
M_{S\to I}(x_2, x_3) \\
P(x_5) \\
V(x_6) \\
C(x_5, x_7) \\
U \\
I(x_7, x_8) \\
B \\
E(x_8)
\end{bmatrix}
+
\begin{bmatrix}
h_{11} & 0 & 0 & \cdots & \uparrow \\
h_{21} & 0 & 0 & & \\
0 & 0 & 0 & & \\
0 & 0 & 0 & \cdots & \mathbf{h}_m \\
0 & +1 & +1 & & \\
0 & 0 & -1 & & \\
0 & 0 & 0 & & \\
0 & 0 & 0 & \cdots & \downarrow
\end{bmatrix}
\begin{bmatrix} \delta Q^\star \\ F \\ D \\ \vdots \\ u_m \end{bmatrix}
$$

n.b. entries $h_{11} = \frac{0.01}{66.90}$ and $h_{21} = \frac{0.01}{168.95}$ are calibration factors such that setting $\delta Q^\star = 1$ corresponds to a 1% increase in insolation.
Inputs: $\delta Q^\star$ represents percentage insolation change; F represents fossil-fuel burning; R represents deforestation.

Figure 4: Expansion of equation (29) $R\dot{\mathbf{x}} = G\mathbf{f}(\mathbf{x}) + H\mathbf{u}$.

The linearisation is valid for small deviations in the states about the equilibrium. In fact, even for larger deviations, such as in Fig. 13, the nonlinear model gave qualitatively similar results.

3.3 Stability Analysis

If the outputs $\boldsymbol{\delta}\mathbf{x}$ of the linearised model are to be stable with respect to the inputs $\boldsymbol{\delta}\mathbf{u}$, then each transfer function $\phi_{\delta u_i \to \delta x_j}$ must be stable. The transfer functions between $\boldsymbol{\delta}\mathbf{u}$ and $\boldsymbol{\delta}\mathbf{x}$ are given by the following standard rearrangement of (31) after taking Laplace transforms:

$$\begin{aligned} s\boldsymbol{\delta}\mathbf{x}(s) &= R^{-1}GF\boldsymbol{\delta}\mathbf{x}(s) + R^{-1}H\boldsymbol{\delta}\mathbf{u}(s) \quad \text{(We begin with } \boldsymbol{\delta}\mathbf{x}\big|_{t=0} = 0\text{)} \\ (sI - R^{-1}GF)\boldsymbol{\delta}\mathbf{x}(s) &= R^{-1}H\boldsymbol{\delta}\mathbf{u}(s) \\ \boldsymbol{\delta}\mathbf{x}(s) &= (sI - R^{-1}GF)^{-1}R^{-1}H\boldsymbol{\delta}\mathbf{u}(s) \\ &:= \Phi(s)_{\boldsymbol{\delta}\mathbf{u}\to\boldsymbol{\delta}\mathbf{x}}\,\boldsymbol{\delta}\mathbf{u}(s) \end{aligned} \tag{32}$$

A sufficient condition for asymptotic stability of our system is therefore that the poles of the entries of the transfer function matrix $\Phi(s)_{\boldsymbol{\delta}\mathbf{u}\to\boldsymbol{\delta}\mathbf{x}}$ lie strictly in the left half-plane, i.e. that the real parts of the solutions s of $\det(sI - R^{-1}GF) = 0$ are strictly negative. Table 2 lists the poles resulting from the linearisation, confirming the asymptotic stability of the system defined. The most important conclusion is therefore that a step input in insolation or CO_2 forcing should result in a transition to a new steady-state, e.g. a higher temperature. For small deviations from the operating point, the linearised model should behave similarly to the non-linear model (see §4).

Table 2 also shows the range of speeds at which the transients decay. The faster transients, associated with the small thermal inertia of the atmosphere and upper ocean, correspond to the changes in the first ten or so years, whereas the slower ones reflect the high thermal inertia of the bulk of the ocean.

3.4 Thermal Cycle Validation

The thermal cycle is validated by comparison with Harvey and Schneider's results. This was achieved by disabling the feedbacks between the carbon and thermal cycles and running a simulation with insolation increased by 2%. The results are shown in Table 3, and the time responses are compared in Fig. 5.

Pole location	Time constant $\frac{1}{\lvert p_i \rvert}$
-2.44$\times 10^{-4}$	4100 years
-4.63$\times 10^{-3}$	215 years
-7.81$\times 10^{-3}$	128 years
-3.23$\times 10^{-1}$	3.1 years
-1.06	0.94 years
-7.33	0.14 years (50 days)
-145 $\pm$ 16.8i	0.0069 years (2.5 days)

Table 2: Poles of the system $\boldsymbol{\delta \mathbf{x}}(s) = \Phi(s)_{\boldsymbol{\delta \mathbf{u}} \rightarrow \boldsymbol{\delta \mathbf{x}}} \, \boldsymbol{\delta \mathbf{u}}(s)$

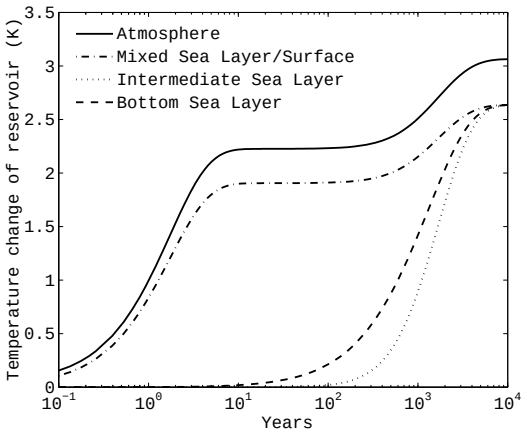

(a) This model

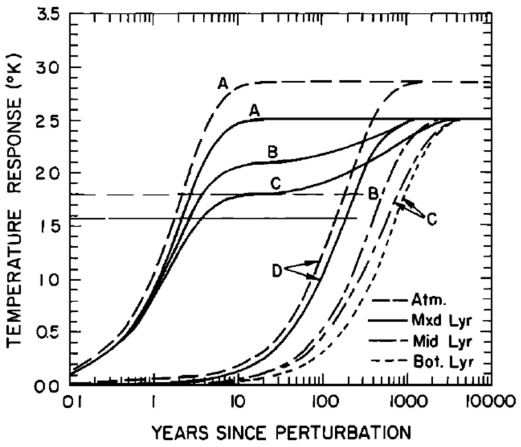

(b) Harvey and Schneider (Curves C, sea layers only)

Figure 5: Perturbation response for a 2% step insolation increase, without carbon cycle coupling. Note that (b) does not show an atmosphere curve corresponding to this case (labelled C).

A fairly close match to these results was achieved. Differences are likely to be down to the treatment of SWR absorption, which [9] did not describe in full. Qualitatively, though, the behaviour of our system is very similar.

ΔT **(K)**	**Output**	**Harvey and Schneider**	**Difference**
Atmos.	3.06	2.83	+8.1%
Sea Layers	2.64	2.46	+7.3%

Table 3: Validation against Harvey and Schneider

3.5 Carbon Cycle Validation

Although long-term validation is difficult due to the lack of studies comparable to this one, the short-term properties of the carbon-cycle can be 'sanity-checked' by comparing

the results of temperature forecasts under CO_2 emissions scenarios with those from literature. This is done in §4.2.2, and confirms that the carbon model implemented produced results in the correct region.

3.6 Equilibrium Conditions

The equilibrium state is defined as $\mathbf{x}_0 = [x_{10} \quad x_{20} \quad x_{30} \quad x_{40} \quad x_{50} \quad x_{60} \quad x_{70} \quad x_{80}]^T$ and is assumed to be the condition at $t = 0$ for all our simulations. An external forcing input such as fossil fuel burning is then to be applied, with the objective in §5 being to investigate the use of state feedback to improve the situation.

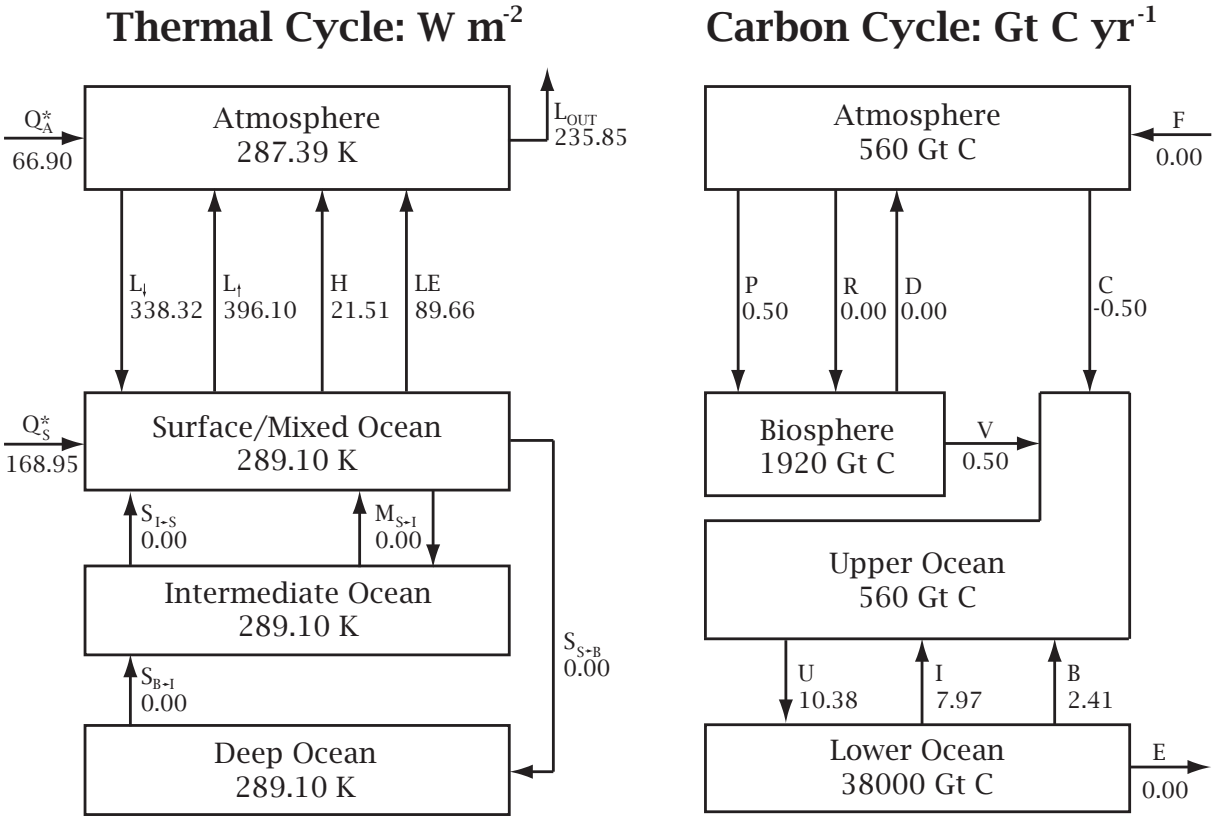

Figure 6: Equilibrium state of the coupled model.

From the diagram above, we have $x_{10} = T_{A0} = 287.39$, $x_{20} = T_{S0} = 289.10$, $x_{30} = T_{I0} = 289.10$, $x_{40} = T_{B0} = 289.10$, and $x_{50} = C_{10} = 560$, $x_{60} = C_{20} = 1920$, $x_{70} = C_{30} = 560$, and $x_{80} = C_{40} = 38000$. The symbols for each transfer process were explained in Table 1.

This equilibrium has been imposed artificially to some extent, particularly in the carbon cycle, which historically has never been in equilibrium due to the continuous transport by rivers. Consequently the carbon cycle rates described above are not entirely

consistent with the equations defined in §2.3.2, and **the carbon equilibrium conditions show very slight deviations from those defined in paragraph above**. When the model is linearised about the operating point $\mathbf{x}_0$, however, the model retains the correct sensitivities to changes in the states and inputs and the validity of the results is preserved.

4 Responses to External Forcing

In this section the response of the model to external forcing inputs will be discussed. This provides a prediction of the effects of human activity (most importantly fossil fuel burning) on the climate according to the model. It also provides a check that the predictions are sensible, in that the results below are compared to some of the many climate forecasts available. In terms of forming judgments on how to tackle climate change, the short term (next 100-200 years) response of the system is of most interest. However, §3.3 has shown that the transient response will last thousands of years before equilibrium. Therefore, as well as running the model to equilibrium, we also check the short-term FFB response.

The following were simulated by setting entries of the matrix H and $\mathbf{u}$ in Equation 31.

4.1 Solar Forcing

The sun's radiation levels vary naturally due to its 11-year sunspot cycle. The magnitude of this variation is around 0.1% of the mean level [25]. Given that the lengths of our simulations are of the order 10,000 years, we will neglect the effects of this phenomenon. Instead, we will concentrate on the effects of a step increase in the incoming solar radiation, and compare our results with those of [9] in order to assess the effects of including a coupled carbon cycle. Fig. 7 shows the model output for a 2% increase in insolation. A similar result was validated for the thermal cycle alone in §3.4, but this test shows that solar forcing also has a significant effect ($\sim$10% increase) on carbon levels in the atmosphere and biosphere.

4.1.1 Effect of Carbon Feedbacks

The effect of coupling the thermal and carbon cycles is to increase the steady-state changes in temperature relative to the uncoupled case. The surface temperature change

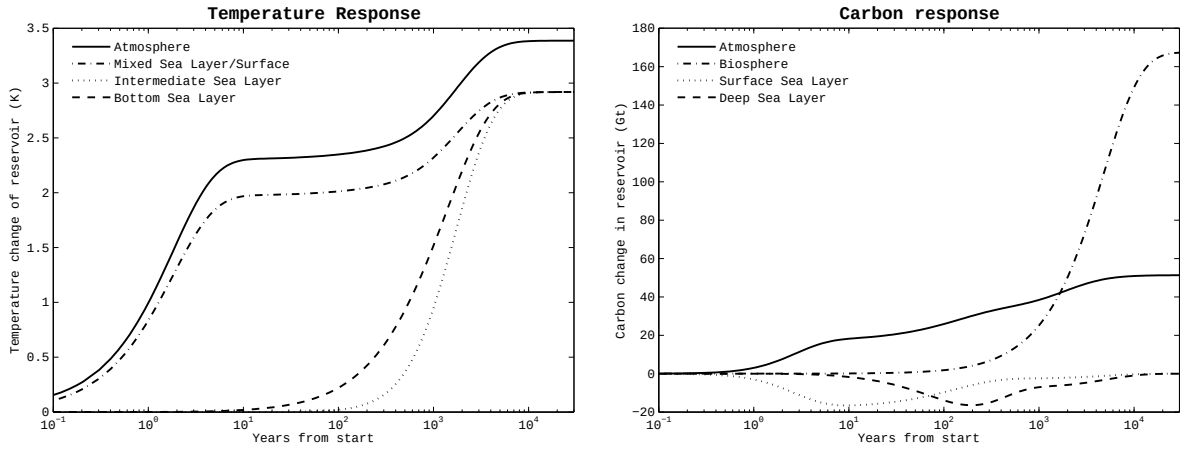

Figure 7: Response to 2% increase in insolation ($\delta Q^\star = 2$)

increased from 2.64 K to 2.91 K (+10.2%), and the atmospheric temperature change increased from 3.06 K to 3.38 K (+10.5%).

4.2 Anthropogenic Carbon Emissions

4.2.1 Emissions Scenarios

From the current rate of between 7 and 8 Gt yr^{-1}, carbon emissions are expected to grow in the near future, and then saturate and decrease as emissions-limiting technologies and policies come into effect. There is much disagreement, however, on how successful these reduction efforts will be, and consequently many researchers have drawn up conflicting predictions of future emissions scenarios. This range is illustrated in Fig. 8. Although all forecasts show an increase until the middle of the 21st century, there is evidently much disagreement on what could happen after that.

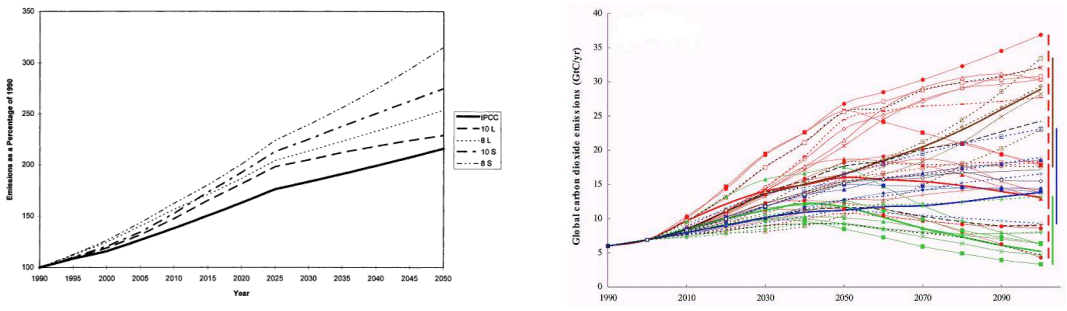

(a) Schmalensee, Stoker, Judson 1998 (b) IPCC WG1

Figure 8: Range of future emissions scenarios, collated by (a) Schmalensee et al. [32] (b) IPCC Special Report [22].

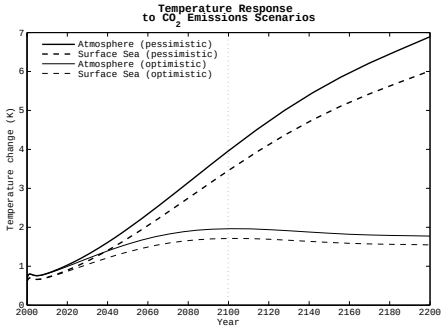

(a) Output of this model from polynomial fits to best-case and worst-case IPCC scenarios

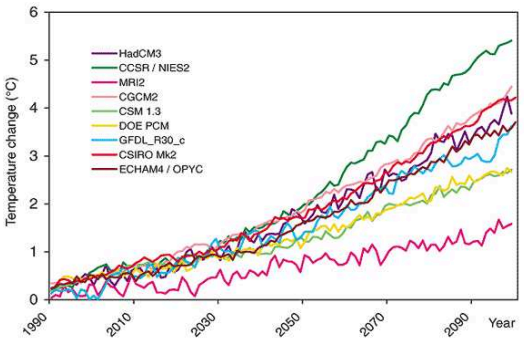

[25]

(b) IPCC WG1 results for various emissions scenarios

Figure 9: Response to CO_2 emissions scenarios: (a) this model vs. (b) IPCC projections

ΔT **at Year 2100**	**This Model**		**IPCC summary**
	Atmosphere	Surface Sea	Atmosphere
Most Optimistic Scenario	**1.96**	1.71	**1.6**
Most Pessimistic Scenario	**3.96**	3.46	**5.3**

Table 4: Comparison of ΔT predicted by this model and by IPCC-collated results

4.2.2 Short-term Response

Fig. 9 shows a comparison between the output of this model and IPCC-collated results from various comparable studies. Table 4 shows that the model predicts temperature rises in broad agreement with those other studies.[14] This is encouraging since the other models used are sure to have been significantly more advanced. The result also serves as validation of the short-term characteristics of the carbon cycle model.

4.3 Deforestation

Fig. 10 shows the response to deforestation of $D = 0.1$ Gt yr^{-1}. Despite this being only about one tenth of the current rate, the steady state level of vegetation (where the increased atmospheric CO_2 is enough to sustain 0.1 Gt yr^{-1} of new plant growth) is almost 400 Gt (around 20%) lower than the initial value. Clearly, though, deforestation has been a rapid human-induced phenomenon with rates varying massively over the last few hundred years: 90% of forest areas in the USA have been cleared since the 17th century. For this reason, and because we have not attempted to include any detail in our biosphere model, few conclusions can be drawn from this result.

[14] n.b. the upper and lower bounds for the IPCC graph do not come from the upper and lower bounds from the IPCC graph in Fig. 8 (b)

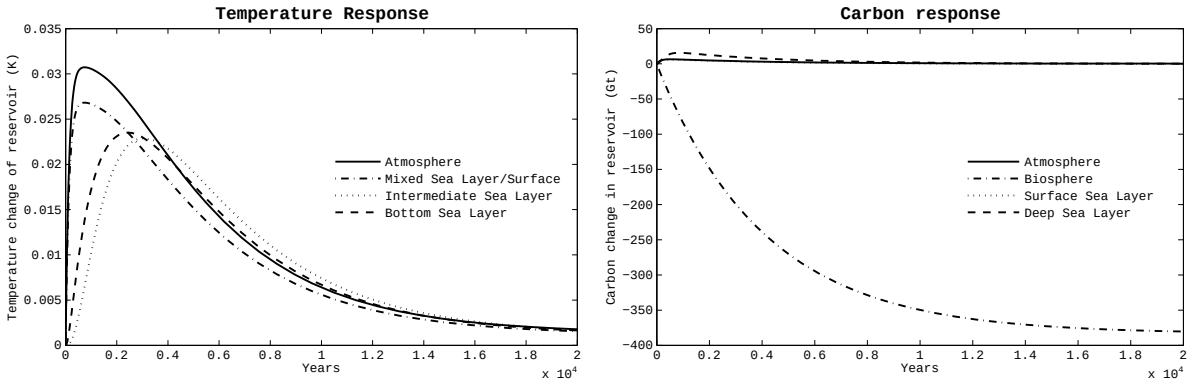

Figure 10: Deforestation response of this model with $D = 0.1$ Gt yr^{-1}.

5 About ACC Schemes

5.1 Recently-discussed Countermeasures

Countless schemes have been suggested as countermeasures both to the warming effect of carbon emissions, and to the problem of reducing the quantities of carbon responsible. They have included:

- Carbon sequestration, also known as carbon capture storage (CCS), either by direct harvest from the atmosphere, or at point of fossil fuel burning. Exhausted oil fields off the coast of Norway are already being exploited for this purpose [2].
- Seeding the ocean surface with nutrients (particularly iron [19]) to encourage the growth of marine biota, in order to pump carbon from the atmosphere to sediment the bottom of the ocean as organisms grow, die and sink . This process is described more fully in §2.3.2.
- Pumping nutrient-rich water from the deep sea to the surface in order to increase the surface layer's capacity to support life, with the same aim of increasing the rate of the biological pump as above. This measure was advocated by Lovelock and Hadley and discussed in the recent press [39, 5, 17].
- The use of a large shield in space (or many smaller shields), for example at the Lagrangian point, in order to block part of the solar incoming radiation, with the aim of stabilising the earth at a lower temperature [3, 36].
- Encouraging cloud formation by depositing sulphate particles or sea spray in the lower atmosphere as nucleation sites [30]. The presence of clouds increases the earth's albedo, thereby decreasing the amount of incoming radiation absorbed.

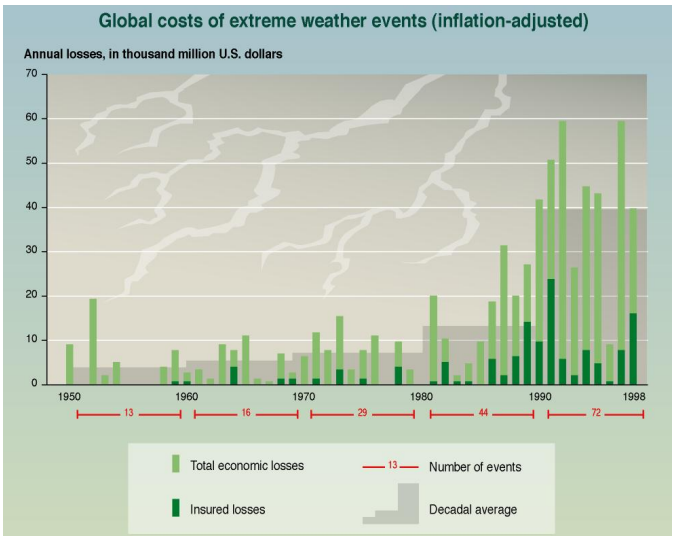

Figure 11: Rising cost of extreme weather events. Source: IPCC WGI 4th Assessment Report [34].

- Deliberately using a technique such as nuclear explosions to send dust into the atmosphere, the cooling effects of which have been studied [29]. Such a cooling effect (thought to be as much as 1.0 °C [26]) was recorded after the eruption of Mount Krakatoa in 1883.

- Even more outlandish schemes include exporting CO_2 to an extraterrestrial location, repositioning the earth's orbit to a path further from the sun, or using government intervention (such as tax incentives) to reduce the earth's population.

5.2 Cost Functions for ACC Schemes

It is theoretically possible, by collating the results of various economic reports on the effects of climate change,[15] to arrive at cost matrices based on the economic effects of climate changes and the cost of ACC schemes. These matrices would be suitable for use in optimisation schemes such as LQR (§6.2). For example, rising air temperatures could be connected to the cost of treating increased disease prevalence; rising oceanic CO_2 could be linked to the economic effects of the disruption of THC, and so on. Fig. 11 demonstrates the rising economic cost of extreme weather events as an example. In theory, by including all reasonable countermeasures in $\mathbf{u}$ and their associated costs in matrix S in equation (36) in the next section, and the state costs in matrix Q, the cheapest course of action in dollar terms would be given by some optimal $\mathbf{u}^{\star}(t)$. However, even assuming costs could be projected accurately, this approach is problematic in practice:

[15] For example the 2006 Stern Review to the British government [35]

1. Predicting abrupt changes in circumstance which could be engendered by climate change, e.g. war or natural disaster, is all but impossible.

2. The scaling of economic costs with temperature and carbon deviations is complex and is likely to be found to be discontinuous (e.g. based on discrete events: diplomatic agreements, exhaustion of resources...) and/or correlated in a way that makes the optimisation difficult to solve.

3. Many proposed ACC schemes have one-off rather than continuous costs - either you build a giant space reflector or you do not.

4. This approach ignores moral responsibility for factors such as reduced biodiversity and displacement of human populations.

Crudely speaking, though, the current debate surrounding climate change policy stems from arguments of minimising future cost, and so pursuing the above process more thoroughly for a more complex class of model would certainly be informative.

5.3 Countermeasures as Model Inputs

Our equations are arranged such that climate control schemes can be represented by model inputs. Carbon transfer processes such as deforestation can be represented by a -1 and $+1$ entry in the H matrix (in the rows corresponding to the source and destination respectively), and the same can be done for heat transfers. Any number of inputs can be added in this way, as shown in the matrix equation of Fig. 4.

6 Solar Dimming

6.1 Back-computing the Control Input

First we rename parts of the model for convenience, so that equation (31)

$$\begin{aligned} \dot{\boldsymbol{\delta}}\mathbf{x} &= R^{-1}GF\boldsymbol{\delta}\mathbf{x} + R^{-1}H\boldsymbol{\delta}\mathbf{u} \\ \text{becomes} \qquad \dot{\mathbf{x}} &= A\mathbf{x} + B\mathbf{u}. \end{aligned}$$

For solar dimming, we will use the solar dimming input $u_1 = \delta Q^\star$ and the FFB input $u_2 = F$.[16] It is more convenient to separate out the B matrix to give the form

$$\dot{\mathbf{x}} = A\mathbf{x} + \mathbf{b}_Q\delta Q^\star + \mathbf{b}_F F. \tag{33}$$

Given a known emissions rate and a known resulting rate of change of the atmospheric temperature, the required input $\delta Q^\star$ can be calculated by taking the relevant row of the state-space equation (31) and solving for $\dot{x}_1 \equiv 0$, i.e. the aim is to hold atmospheric temperature constant:

$$\dot{x}_1 = \sum_{i=1}^{8} a_{1i}x_i + b_{Q1}\delta Q^\star + b_{F1}F = 0$$

for all $\mathbf{x}$ and t. From Fig. (4), $h_{F1} = b_{F1} = 0$ means we can set

$$\begin{aligned} \delta Q^\star &= -\frac{\sum_{i=1}^{8} a_{1i}x_i}{b_{Q1}}, & (34) \\ \text{so that } u &= -K_{bc}\mathbf{x} & (35) \end{aligned}$$

where $K_{bc} = \frac{\langle A\rangle_1}{b_{Q1}}\mathbf{x}$, and $\langle A\rangle_1$ is the first row of A. The scheme is shown in Fig. 12. Since F does not enter into the top line of the equation, we do not need to know its value to stabilise x_1. Similarly, for constant surface temperature, $\dot{x}_2 = 0$ can be set by replacing $\langle A\rangle_1$ with $\langle A\rangle_2$ and b_{Q1} with b_{Q2}.[17] However, we cannot use this technique to control any states other than x_1 or x_2 since only the first two elements of $\mathbf{b}_Q$ are non-zero. Another drawback of this method is that we cannot use it to correct an existing

[16] Note that for convenience we will use $\mathbf{x}$ instead of $\boldsymbol{\delta}\mathbf{x}$ to represent deviations from the equilibrium from now on.

[17] Moreover, we can specify any differentiable time response $\chi(t)$ in x_1 or x_2 by adding $\frac{\chi'(t)}{b_{Q\{1,2\}}}$ to the input.

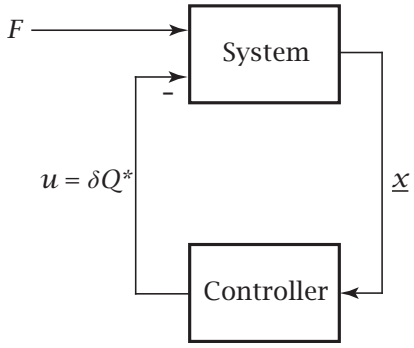

Figure 12: Back-computation scheme, equation (35).

temperature offset to zero.[18] This is confirmed by looking at the poles of the closed-loop system, which are given by the eigenvalues of $A - \mathbf{b}_Q K_{bc}$, where $K_{bc} = \frac{\langle A \rangle_1}{b_{Q1}}$. The first row of $A - \mathbf{b}_Q K_{bc}$ evaluates to $\langle A \rangle_1 - b_{Q1} \frac{\langle A \rangle_1}{b_{Q1}} = [0 \ \cdots \ 0]$, i.e. a zero row giving a pole on the origin; therefore the system is only marginally stable and will not reject an initial temperature offset asymptotically. It will also give poor performance or instability in the case of disturbances such as sunspot activity.

Fig. 13 shows that where the model is error-free and equation (34) gives no offset in $\dot{x}_1$ (§6.3 discusses the case where there is error), the scheme succeeds in holding x_1 constant, and holds all temperatures near their initial values, but has virtually no improving effect on the carbon cycle. A conclusion that can be drawn from this is that **solar dimming in practice does nothing about those CO_2 problems which are unrelated to warming**, for example ocean acidification [10].

A steady-state dimming of about 1.5% insolation counteracts the warming effect of burning fossil fuels at a rate of 5 Gt yr^{-1}, a rate chosen to represent a small eventual reduction from the current FFB rate. By an energy balance argument, it is clear that *any* control rule for system (33) will give the same result once steady state has been reached. This is certainly in the region of the 2% dimming which Teller predicted to be necessary [36], and Angel's calculation of 1.8% [3], although these results were based on their own (similar) FFB forecasts. By way of comparison, the IPCC WGI reported [25] that human action is already responsible for a reduction of up to 4% of solar energy reaching the earth's surface, due to particles released into the atmosphere. However since this energy is absorbed by particles in the atmosphere itself rather than outside it, as is the case with a space shield, this apparent dimming cannot be exploited to produce a cooling effect.[19]

[18] Even if we choose a trajectory χ as in footnote 17, it will not be apparent whether a more optimal one could be chosen.

[19] ACC schemes relying on putting particles in the atmosphere rely on putting them at much higher altitudes, and would scatter much of the radiation upwards rather than absorb it.

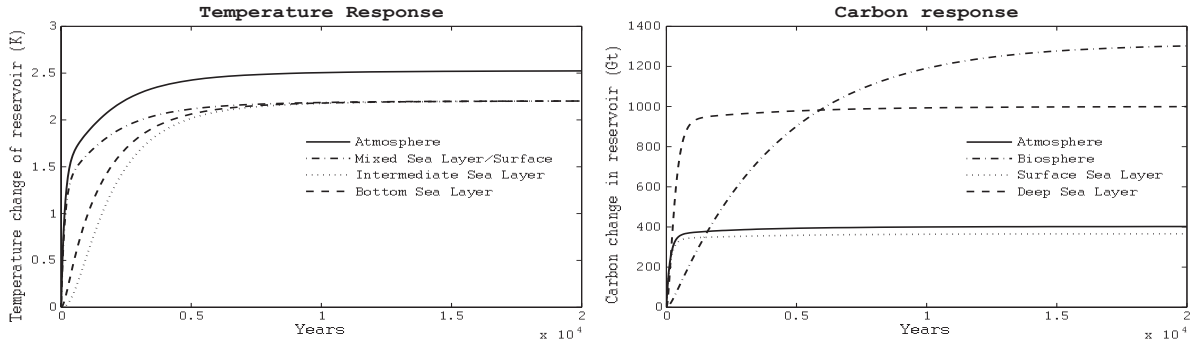

(a) No control input

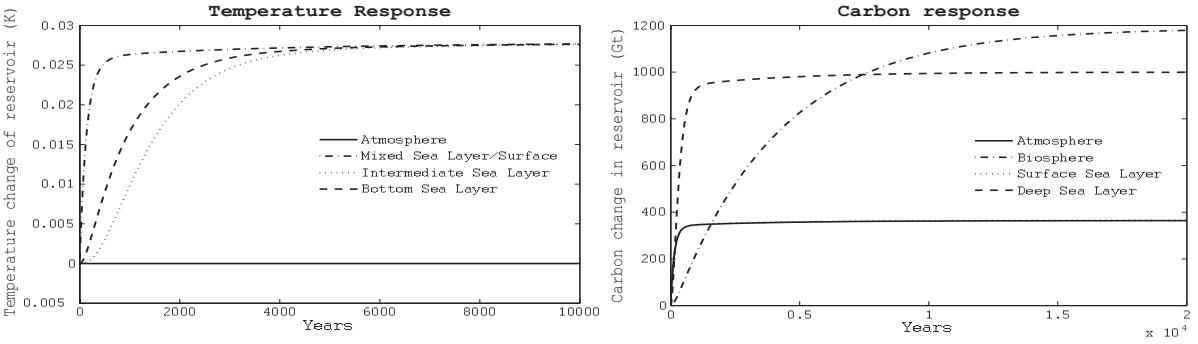

(b) Maintaining T_A constant

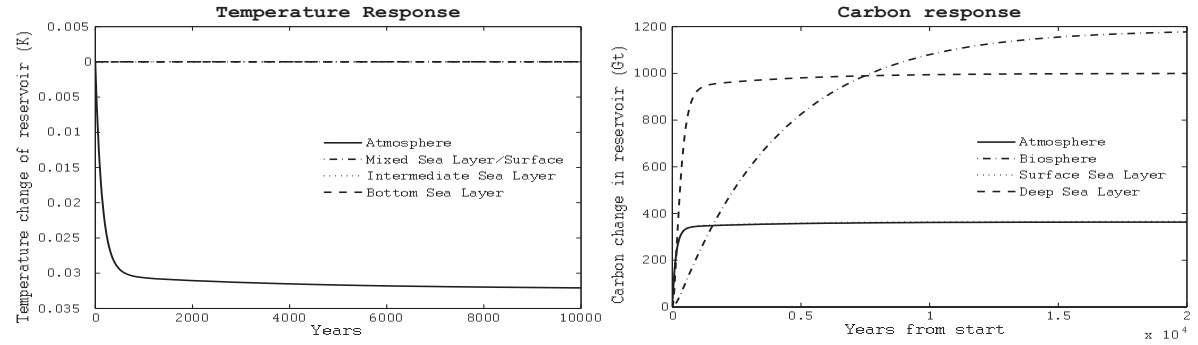

(c) Maintaining T_S constant

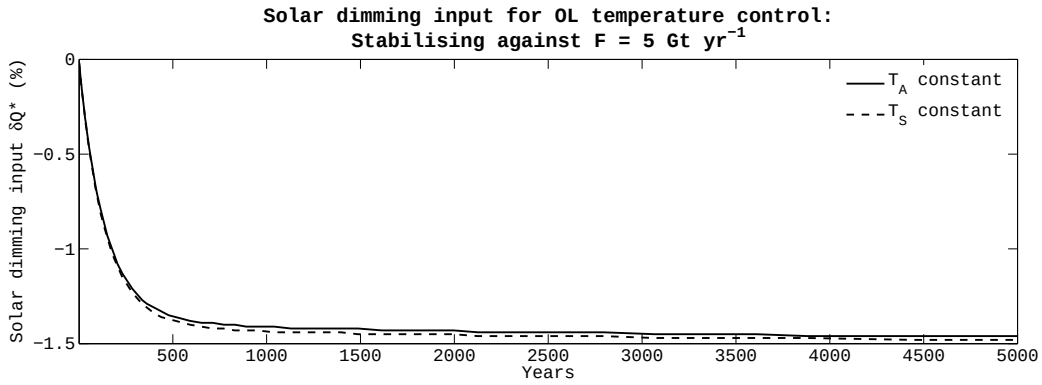

(d) Control input $\delta Q^\star$ for (b) and (c)

Figure 13: Back-computed solar dimming with F = 5 Gt yr^{-1}. Although all simulations were run for 20,000 years, some time axes have been truncated so that trends can be seen more clearly.

6.2 LQR Control

6.2.1 Temperature Regulation as an LQR Problem

The challenge of maintaining global temperatures at their "initial" (pre-industrial) state for the least effort can be framed as an Linear Quadratic Regulator problem: given matrices Q and R,[20] which represent weighted costs of non-zero $\mathbf{x}$ and $\mathbf{u}$ vectors, determine an optimum $\mathbf{u}^\star(t)$ to minimise the cost V given by

$$V = \int_{t=0}^{\infty} \mathbf{x}(t)^T Q \mathbf{x}(t) + \mathbf{u}(t)^T R \mathbf{u}(t) \ \mathrm{d}t \tag{36}$$

In this case, $\mathbf{u}^\star = -K_{lqr}\mathbf{x}$ will be will be a state-feedback[21] controller giving optimal disturbance rejection based on weightings Q and R. The controller is defined by

$$K_{lqr} = R^{-1} B^T P \tag{37}$$

where P solves the continuous-time algebraic Riccati equation

$$A^T P + PA - PBR^{-1}B^T P + Q = 0$$

For solar dimming without FFB, $\mathbf{u}$ is just a scalar $u = \delta Q^\star$, R is a scalar and K_{lqr} is an 8-element row vector.

6.2.2 Solar Dimming for Temperature Regulation

Given non-zero initial temperatures, the above optimisation can be applied to a single solar dimming input $\delta Q^\star$ as defined in §6.1, to return T_A to zero at minimum cost. We set $Q = \mathrm{diag}\,\{1, 0, 0, 0, 0, 0, 0, 0\}$ in order to penalise only T_A, and $R = 1$.[22] Starting from an initial temperature offset,[23] we are then able to regulate the temperatures back to zero, as shown in Fig. 14. However, this assumes that whatever forcing that caused the temperature change has now stopped. A more realistic regulation case is where FFB takes place at the same time (i.e. $F \neq 0$). This is more difficult since we now have an

[20] Note that the R defined here is not related to the heat-capacity matrix R first defined in equation (29), which was subsumed into matrices A and B.

[21] We assume all states can be measured or estimated at sufficiently close time intervals.

[22] R is in fact set by trial and error in order to keep the magnitude of the input $\delta Q^\star$ reasonably small: because of the practicalities of building a large space shield, the scheme is only remotely possible if $-2 < \delta Q^\star < 0$.

[23] We use the steady-state values under carbon emissions of 5 Gt yr^{-1}, as shown in Fig. 13 (a).

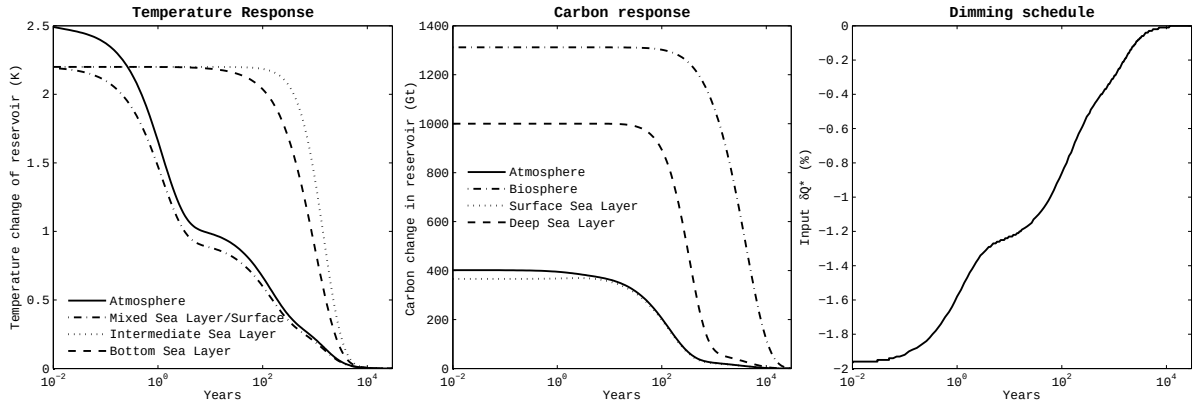

Figure 14: LQR regulation of the temperatures and carbon levels with $F = 0$, after an initial disturbance.

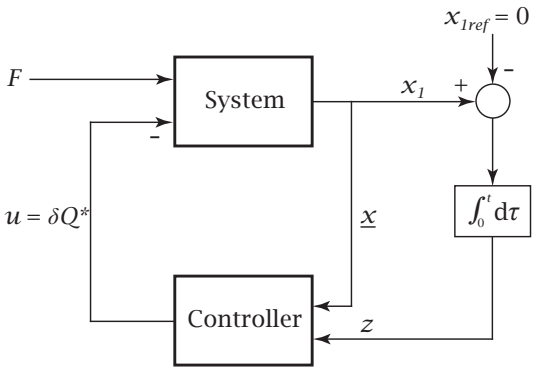

Figure 15: Integral action control scheme, equation (39).

offset on $\dot{C}_1 = \dot{x}_5$ that must be rejected asymptotically. Clearly the solar dimming input $\delta Q^\star$ alone cannot be used to set the whole state vector to zero.[24] Therefore the best we can aim for is $T_A = x_1 = 0$, i.e. we want to get close to the result of the case described in §6.1. Appending F to give a new state vector $\tilde{\mathbf{x}}_1 = [\mathbf{x}^T \; F]^T$ does *not* help:

$$\begin{bmatrix} \dot{\mathbf{x}} \\ \dot{F} \end{bmatrix} = \begin{bmatrix} A & \mathbf{b}_F \\ 0 & 0 \end{bmatrix} \begin{bmatrix} \mathbf{x} \\ F \end{bmatrix} + \begin{bmatrix} \mathbf{b}_Q \\ 0 \end{bmatrix} \delta Q^\star \; := \tilde{A}_1 \tilde{\mathbf{x}}_1 + \tilde{\mathbf{b}}_1 u \tag{38}$$

An LQ regulator *cannot* be found because $(\tilde{A}_2, \; \tilde{\mathbf{b}}_2)$ is not controllable (this is obvious since we cannot influence the value of F): we cannot hope to regulate the whole state to zero using such an arrangement. Instead we include integral action $\int_0^t T_A \, \mathrm{d}\tau$ in the controller, as shown in Fig. 15. We append the variable z to the state vector such that $\dot{z} = x_1$. We then form a new state vector $\tilde{\mathbf{x}}_2 = [\mathbf{x}^T \; z]^T$:

$$\begin{bmatrix} \dot{\mathbf{x}} \\ \dot{z} \end{bmatrix} = \begin{bmatrix} A & \mathbf{0} \\ 1 \; 0 \cdots 0 & 0 \end{bmatrix} \begin{bmatrix} \mathbf{x} \\ z \end{bmatrix} + \begin{bmatrix} \mathbf{b}_Q \\ 0 \end{bmatrix} \delta Q^\star + \begin{bmatrix} \mathbf{b}_F \\ 0 \end{bmatrix} F \; := \tilde{A}_2 \tilde{\mathbf{x}}_2 + \tilde{\mathbf{b}}_2 u + \tilde{\mathbf{b}}_F F \tag{39}$$

[24] For the system $\dot{\mathbf{x}} = A\mathbf{x} + \mathbf{b}_F F + \mathbf{b}_Q \delta Q^\star$, setting $\mathbf{x} = 0$ at steady state requires $\mathbf{b}_Q \delta Q^\star = -\mathbf{b}_F F$, which is impossible unless $\delta Q^\star = F = 0$.

We require a new 9×9 matrix $\tilde{Q} = \text{diag}\{1, 0, 0, 0, 0, 0, 0, 0, 0\}$ to fit the augmented state-space, but we try not to penalise z, which has little physical significance. $R = 1$ as before. Although we cannot form an LQ regulator from the new set ($\tilde{A}_2,\ \tilde{\mathbf{b}}_2,\ \tilde{Q},\ R$),[25] we can add a small amount of integral feedback to the K_{lqr} row vector defined above, so that we obtain

$$u = -\tilde{K}_{lqr}\tilde{\mathbf{x}}_2 = -\begin{bmatrix} K_{lqr} & \epsilon \end{bmatrix}\begin{bmatrix} \mathbf{x} \\ z \end{bmatrix}. \tag{40}$$

We set ϵ, the rate of integrator wind-up, to a small value[26] $\epsilon = 0.03$. We also require the new controller to be asymptotically stable in order to reject the non-zero initial condition, a sufficient condition for which is that the eigenvalues of $\tilde{A}_2 - \tilde{\mathbf{b}}_2\tilde{K}_{lqr}$ have negative real parts. This is the case as long as $\epsilon > 0$.

Starting from the initial offset described in footnote 23, the controller was applied with and without the effects of the integral action. The two cases are shown in Fig. 16 (a) and (b). Without integral action the controller fails to set $x_1 = 0$ for non-zero F. Fig. 16 (c) shows the result of using a simpler dimming schedule ending on the same required steady-state value: we see that if a full capacity of 2.12% dimming is to be used, it is better to apply it straight away (i.e. it would not produce unwanted extra cooling). Note that calculating these simplified schedules has required a forecast to the maximum (red line) and final (blue line) input values, which would not be possible if the FFB rate were constantly changing. This justifies the use of a control scheme such as the one described above.

6.3 Effect of uncertainty

To illustrate the effects of having an uncertain parameter in the model, the controllers were calculated as above, and then matrix F was changed to reflect a level of radiative forcing 10% higher than predicted by equation (23). Fig. 17 shows that this results in a slow exponential increase in temperatures for the back-computation controller, whereas the LQR controller modified with integral action corrects for the error. For the back-computation controller, we can see that exponential growth takes place by considering the matrix equation with A modified to include an additive error Δ. Equation (33) becomes, after substituting in the control law (35), $\dot{\mathbf{x}} = (I + \Delta)A\mathbf{x} + \mathbf{b}_Q\delta Q^\star + \mathbf{b}_F F$.

[25] This technically requires that the pair ($\tilde{Q}^{\frac{1}{2}},\ \tilde{A}_2$) be detectable, which will only be the case if the bottom-right entry of $\tilde{Q}$ is non-zero. We can therefore form a controller if we penalise integrator wind-up slightly by setting $\tilde{Q} = \text{diag}\{1, 0, 0, 0, 0, 0, 0, 0, \gamma\}$ with $\gamma \ll 1$, but the solution will tend to $[K_{lqr}\ 0]$ as γ tends to zero.

[26] This is in order to keep the magnitude of $\delta Q^\star$ small, but large enough that the feedback is sufficiently fast. A suitable value was found by trial and error.

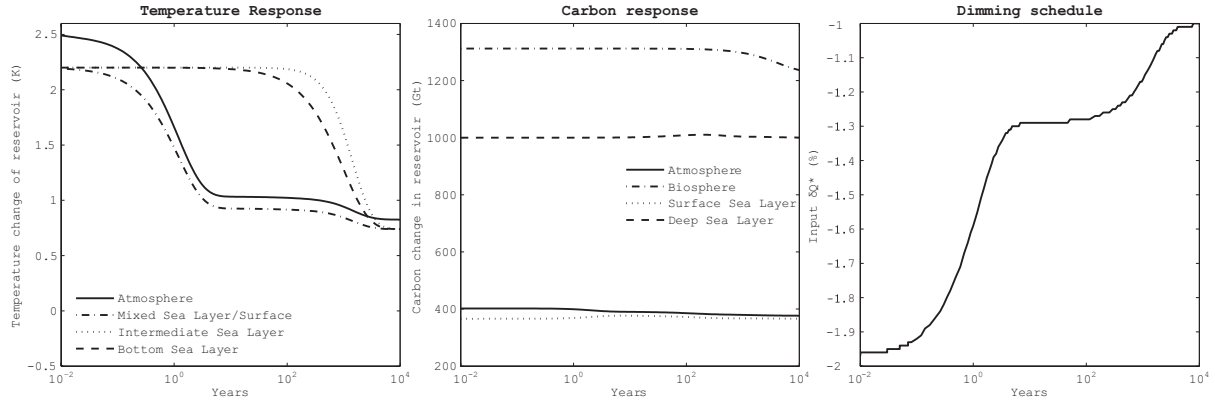

(a) No integral action.

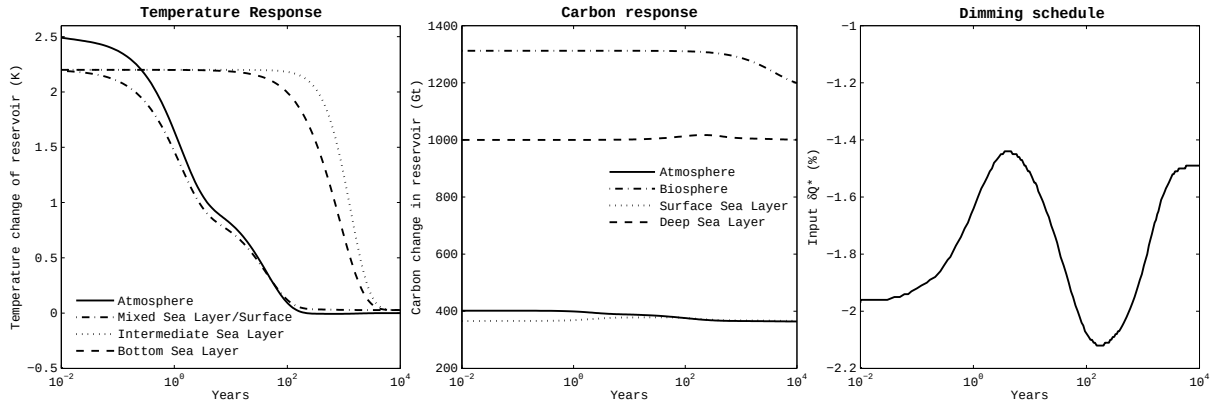

(b) With integral action.

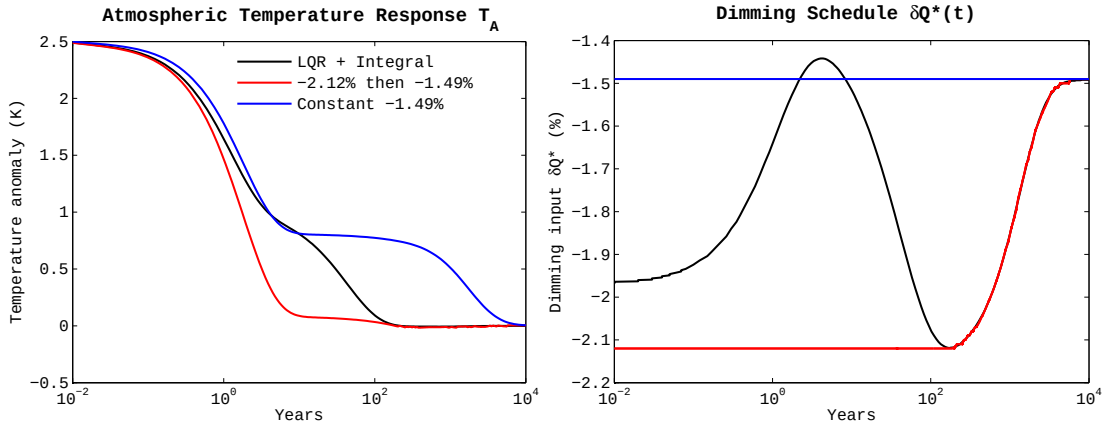

(c) Comparison of dimming schedules.

Figure 16: Dimming for constant $F = 5$ using LQR. $Q = \text{diag}\{1, 0, \ldots, 0\}$; $R = 1$; $\epsilon = 0.03$. With integral action, the excess in T_A is reduced to zero within ∼100 years. In both (a) and (b), biosphere carbon stabilises after around 10^4 more years; all other variables have reached steady state within the axes. (c) shows the response when the input is simplified to more practical schedules.

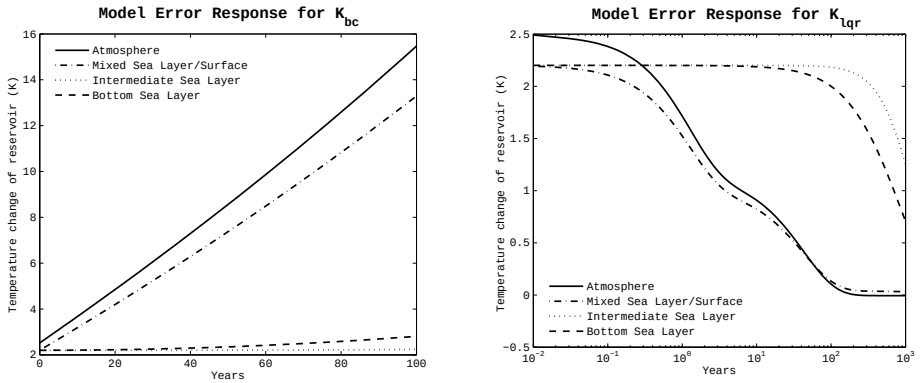

(a) (b)

Figure 17: Comparison of the effects of uncertainty (radiative forcing was made 10% more severe than the assumed level the controller was based on) when the climate is controlled by (a) back-computation and (b) LQR with added integral action.

The first row of this matrix equation evaluates to

$$\begin{aligned} \dot{x}_1 &= \langle (I+\Delta)A\rangle_1 \mathbf{x} - \langle A\rangle_1 \mathbf{x} + 0 \times F \\ &= (\langle A\rangle_1 + \langle \Delta A\rangle_1 - \langle A\rangle_1)\mathbf{x} \\ &= \langle \Delta A\rangle_1 \mathbf{x} \end{aligned}$$

where $\langle\cdot\rangle_1$ again indicates the first row of the matrix or matrix product. The solution will grow exponentially over time if the right hand side of the equation is positive. In this case, increasing radiative forcing does produce a positive RHS, so solution grows as shown in Fig. 17 (a).

7 Other ACC Schemes

Although this report has focused on solar dimming, other ACC schemes from §5.1 may be tested using the model. Two of these schemes are discussed here. Some schemes, such as cloud-seeding, would require an elaboration of the SWR scheme ($\delta Q_A^\star$ and $\delta Q_S^\star$) before they could be implemented, since we have wrapped these effects up into single variables.

7.1 Seawater Pumping

A scheme advocated by Lovelock and Rapley [17] involves pumping water from the deep sea to the surface using cheap, passive wave-powered pumps and valves. Bringing

nutrient-rich water to the surface would remove a bottleneck on the rate of biological activity, which effectively converts dissolved surface-water CO_2 into solid organisms. This amounts to increasing the rate of the biological pump U (described in §2.3.2). With reference to equation (31) we can add an input δU with corresponding column in H given by $\mathbf{h}_U = [0\ 0\ 0\ 0\ 0\ 0\ -1\ +1]^T$. Ignoring the consequences for ocean biodiversity, it is thought that the scheme could be carried out at reasonable cost. Therefore, assuming we know the relationship between this pumping and the change δU in the biological pump rate, we can envisage a scenario as shown in Fig. 18, where seawater pumping compensates for 'business-as-usual' FFB.

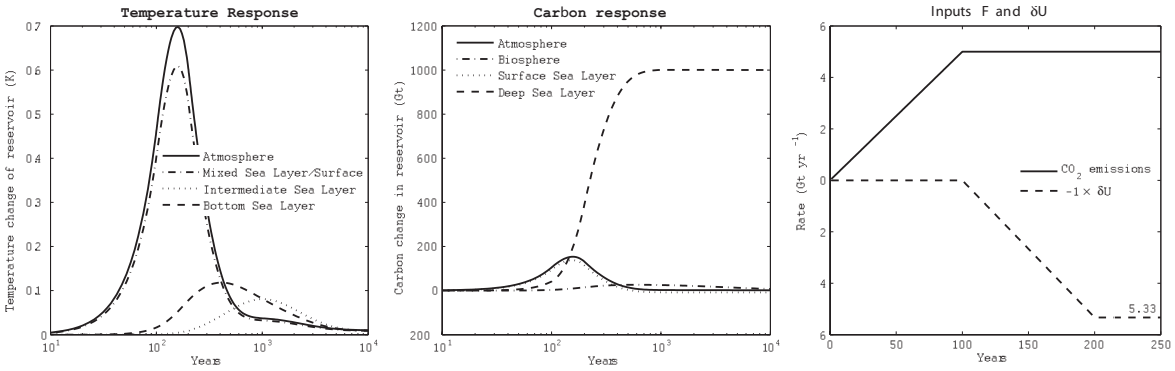

Figure 18: Forecast of temperature and carbon changes under a seawater pumping scheme to compensate for CO_2 emissions. The input scenario is shown by the rightmost graph.

7.2 Carbon Sequestration

Carbon sequestration schemes store carbon either by direct harvest from the atmosphere [15] or at point of FFB (such as [2]). Assuming a well-mixed atmosphere so that these two things are equivalent, then these schemes essentially amount to a negative offset to our FFB input F. Therefore the solution that minimises warming is trivial: just ramp up sequestration efforts until the rate matches that of total FFB (so that effectively $F = 0$),

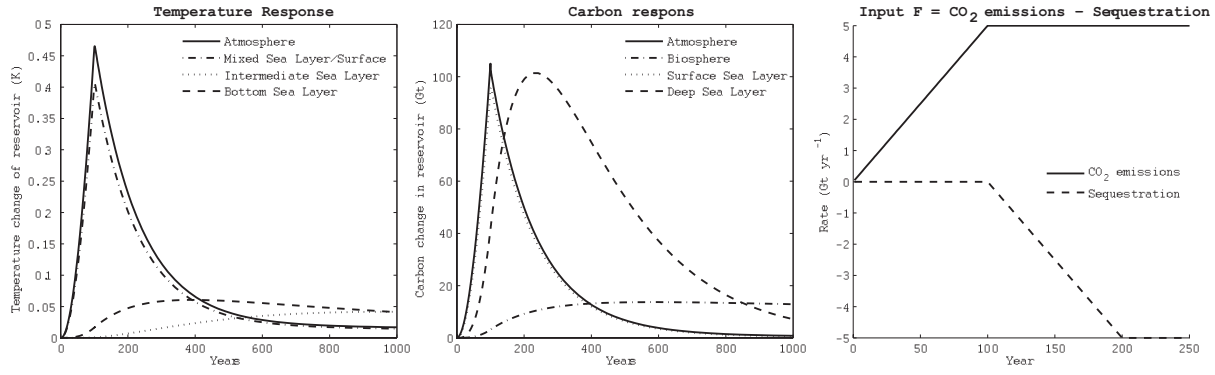

Figure 19: Temperature and carbon forecast under the carbon emission and sequestration scenario described by the rightmost graph.

and according to this model the climate will return to its pre-industrial state, since it is asymptotically stable with zero input. The physical explanation is that excess carbon will eventually leave the system by sedimentation to the sea bed. Fig. 19 shows an example of a scenario like this.

8 Discussion

8.1 Conclusions

A globally-averaged box-model was developed to represent both the thermal activity and carbon transfers within the earth's climate system. It was shown that both the temperature and (short-term) carbon responses compared well to other models in literature. The temperature response was tested by comparing insolation forcing results with Harvey and Schneider's paper, and showed a 10% deviation; the carbon response was tested by comparing FFB-induced temperature changes with forecasts collated by the IPCC, and these results fell within the range of IPCC forecasts. The deforestation response was also tested, and although the conclusion was made that deforestation prompts virtually no temperature increase, the forecast was, as expected, of little practical relevance given the complexity needed to model this effect convincingly. As is the case with many engineering applications, a very simple model was shown to provide reasonable predictions of deviations from equilibrium, even though the equilibrium state itself was not entirely realistic.

The main motivation of the project was to cast climate stabilisation as a control problem. In particular, two control schemes for solar dimming to counteract the effects of FFB were presented. The first, where a controller was designed to hold atmospheric or surface temperatures exactly constant, showed that a ramping-up to almost 1.5% dimming in around 500 years was sufficient. This compared well to the results of Teller (2%) and by Angel (1.8%). However the scheme would not be able to correct an initial temperature offset, and it was explained that model error in the controller could result in an exponential increase in temperatures, which is obviously undesirable. In the second scheme a linear quadratic regulator was implemented. Testing the case where FFB stops after an atmospheric temperature rise of 2.5 °C, the controller corrected to within 0.5 °C after about 100 years. However, where FFB continued the LQR controller would give a steady-state error. This was fixed by including integral feedback in the control law. Under FFB at 5 Gt yr^{-1}, perhaps an attainable rate once a 2.5 °C rise has taken place, it was shown that atmospheric temperature anomaly could be eliminated

using a dimming input which varies over time but barely exceeds 2% dimming. Using a dimming of more than 1.5% at the start was shown to be beneficial in cooling the atmosphere and surface sea's smaller thermal mass. The variation is compatible with Angel's rough calculation that members of a cloud of space shields would have a lifetime of about 50 years, allowing for renewal at a variable rate that can be used to set the dimming schedule. However, as well as showing that the scheme is capable of stabilising temperatures, the simulations also showed that even though dimming can counter the warming effects of increased atmospheric CO_2, it cannot mitigate any other associated problems, since it has almost no effect on carbon cycle dynamics. Carbon sequestration and seawater pumping were shown to be effective in this regard.

A key difficulty in the project has been determining when to investigate the parameterisation of a particular process further and when to cast aside objections and stick to the current simplification. There are endless quantities of climate modelling literature which could have been consulted in this process, and the project has been a perpetual trade-off between rigour and progress. Further work as discussed below, therefore, has scope for both revisiting the work already done, and building on it.

We set out to determine whether, given a simple climate model, we could apply control theory and solve an interesting problem regarding the implementation of ACC schemes. To some extent this aim has been fulfilled, as useful points were made about control for solar dimming, but for many of the schemes it was not even necessary to carry out detailed testing to see that in fact the solutions are obvious: simply apply as great a compensating input as feasible to counteract FFB (this was especially trivial in the case of carbon sequestration, since the input acts in direct opposition to FFB). However, the model itself is still useful in that quick simulations of a range of forcing/compensating scenarios can be made, with results moderately representative of the real system. In addition, we could expand the model as detailed below in order to investigate a richer source of control problems in future.

8.2 Future Work

1. The effects of other ACC schemes listed in §5.1 can be modelled and evaluated more thoroughly than the brief checks that were carried out in §7, as can optimal combinations of these schemes. In order to solve this optimisation problem, it would be necessary to research cost projections of the different schemes, in the manner discussed in §5.2. Since most of the project was spent developing a useful model, there was not enough space to cover a full comparison of schemes here.

2. Make sensitivity studies into the effects of model error, which are a significant source of doubt when it comes to formulating a climate change policy. Expanding more rigorously on §6.3 would be helpful, since if the results change dramatically based on a small variation in a poorly-understood physical process, then it would become clear that basing an ACC scheme on these results would be unwise!

3. Split the model into more geographical regions in order to improve the validity of simulation result and allow simulations of many more schemes and effects. One option would be to include polar regions and distinguish between the northern and southern hemispheres, as is the case in [8]. This would allow a more realistic treatment of the THC, and of polar ice. The advantage of this simple modelling scheme is that as long as the properties assumed before (such as time invariance) hold, the resulting output should be more accurate and no more difficult to evaluate from a control systems perspective. As more detail is developed, it may well be possible to identify interesting trade-offs and investigate the resulting control strategy.

4. Include further cycles, especially the hydrological cycle, but also sulphur, nitrogen and phosphorous. The former is important because it allows the modelling of precipitation, ice caps, glacial flow, and ocean currents. The latter three are important because they impact plant growth and GHG activity in the atmosphere. The matrix equation can be expanded from the current thermal-carbon system without making the theory applied any more complicated.

5. An result of implementing point 4 is that more outputs of concern, such as acid rain (as a function of SO_2 levels) and sea-level rise (from the state of the hydrological cycle), could be extracted as functions of the expanded state vector e.g. $\mathbf{y} = C\mathbf{x}$. At present we are only examining the state directly, so that if anything we have $C = I$. These outputs could then easily be used for calculating new cost functions: LQR minimises $\mathbf{x}^T Q\mathbf{x}$ over time, but for $\mathbf{y} = C\mathbf{x}$ we can just minimise $\mathbf{y}^T Q\mathbf{y} = \mathbf{x}^T C^T QC\mathbf{x} = \mathbf{x}^T Q'\mathbf{x}$.

6. Attempt to relax some of the assumptions made, in order to strengthen the conclusions. For example, in order to model the shrinking of the polar ice caps it would be necessary to bring in seasonal variations (to model freezing and melting cycles). It may then be useful to implement a linear time-varying (LTV) model, which may then yield interesting (non-trivial) control problems for ACC schemes. For example, consider localised dimming for an expanded model as described in point 3 above: although global warming effects are most severe at the equator, one may find advantages in applying seasonal dimming at the poles to prevent sea ice melting and sea-level rise.

9 Appendix

Calculation of Shortwave Absorptions $Q_A^\star$ and $Q_S^\star$

The model used to calculate the globally-averaged shortwave absorptions $Q_A^\star$, the total SWR absorbed in the atmosphere, and $Q_S^\star$, the total SWR absorbed by the planetary surface, as a function of latitude and atmospheric temperature, is detailed as an appendix in Thompson and Barron [37]. However, the method presented there leads to an expression for the overall planetary albedo α_P as a function of latitude. Therefore a slightly different treatment of the model, described here, was needed to extract the values $Q_A^\star$ and $Q_S^\star$, which are related to α_P by

$$\alpha_P = \frac{Q_{OUT}}{Q_{IN}} = 1 - \frac{Q_A^\star + Q_S^\star}{Q_{IN}}.$$

This section necessarily reproduces some of the detail from Thompson and Barron's appendix (the diagram here in particular is very closely based on theirs) in order to explain the new treatment.

The rate of energy absorption by the atmosphere and surface for a given location will depend on:

- Whether there is cloud cover
- Latitude (affects the angle of incidence and hence atmospheric absorption)
- Time of day and time of year
- Surface albedo (a function of sea fraction, terrain type etc.)
- Air temperature

Table 1 of Thompson and Barron, reproduced for convenience as Table 5 of this report, gives data for 10° latitude bands starting at $\theta = -85°$ and ending at $\theta = +85°$.[27] Clearly some assumptions are needed to simplify the model. The first of these is to ***assume equinox conditions***, i.e. that the earth's tilt is such that all parts of the earth experience a 12-hour day. This greatly simplifies the use of equations from p. 15 of Sellers' book

[27] This is because the equations used by Thompson and Barron are not valid for $|\theta| > 85°$, and because the areas subtending those polar extremes only constitute 0.4% of the earth's surface. Note that the proportion of the total solar energy received by these polar areas is even smaller than this.

Latitude	Mean Annual Insolation (W m^{-2})	Ocean Fraction	Sea Ice Fraction	Mean Annual Temperature (K)	Cloud Fraction	Base Zonal Land Albedo
85-75N	179.0	.81	.90	258.2	.64	.16
75-65	197.8	.45	.50	264.1	.66	.16
65-55	237.5	.38	.14	272.1	.69	.16
55-45	285.5	.42	.00	278.3	.67	.16
45-35	329.9	.54	.00	285.7	.60	.16
35-25	367.7	.59	.00	292.9	.52	.20
25-15	394.8	.68	.00	298.1	.41	.25
15-5	411.9	.76	.00	299.6	.47	.15
5N-5S	417.7	.77	.00	299.4	.49	.12
5-15	411.9	.78	.00	298.7	.48	.14
15-25	394.8	.76	.00	296.4	.46	.18
25-35	367.0	.81	.00	292.3	.49	.16
35-45	329.9	.95	.00	286.5	.58	.16
45-55	285.5	.98	.00	279.5	.73	.16
55-65	237.5	1.00	.26	272.3	.81	.16
65-75	197.8	.62	.69	256.0	.67	.16
75-85S	179.0	.07	1.00	234.8	.47	.16

Table 5: Present-day earth climate data for 10° latitude bands, reproduced from Thompson and Barron

[33] to calculate $Z(\theta)$, the mean solar angle of incidence during a day spent at latitude θ. The deviation from the true seasonal weighted average result should not be significant, due to the symmetry between the northern and southern hemispheres. Given time, a more comprehensive orbital calculation along the lines of [4] could have been made.

The next step is to consider clear- and cloudy-sky models in parallel, and combine their outputs as a weighted average. The methods for calculating $Q_A^\star$ and $Q_S^\star$ differ significantly between the clear- and cloudy-skies case, because the cloudy-skies case counts multiple reflections of radiation between the cloud layer and the earth's surface. The models for the two cases, adapted from Thompson and Barron, are shown in Fig. 20. Squares in this figure represent a fractional loss of radiation energy as the radiation passes through. In both cases, the conservation rule for **unit-intensity incident radiation**

$$Q_{OUT} + Q_A^\star + Q_S^\star = 1 \tag{41}$$

is followed, where Q_{OUT} is the component that is re-emitted to space following absorptions and reflections. In the equations that follow, we add the contributions to the total atmospheric SWR absorption $Q_A^\star$ and the total surface SWR absorption $Q_S^\star$. This is done by taking a weighted average of the clear-skies case (equations (42) and (43)) and the cloudy-skies case (equations (44) and (45)). A superscript "$\prime$" indicates that a quantity relates to direct (unscattered) radiation, whereas a "$\star$" indicates a quantity relating to diffuse radiation (scattered or having passed through the cloud layer).

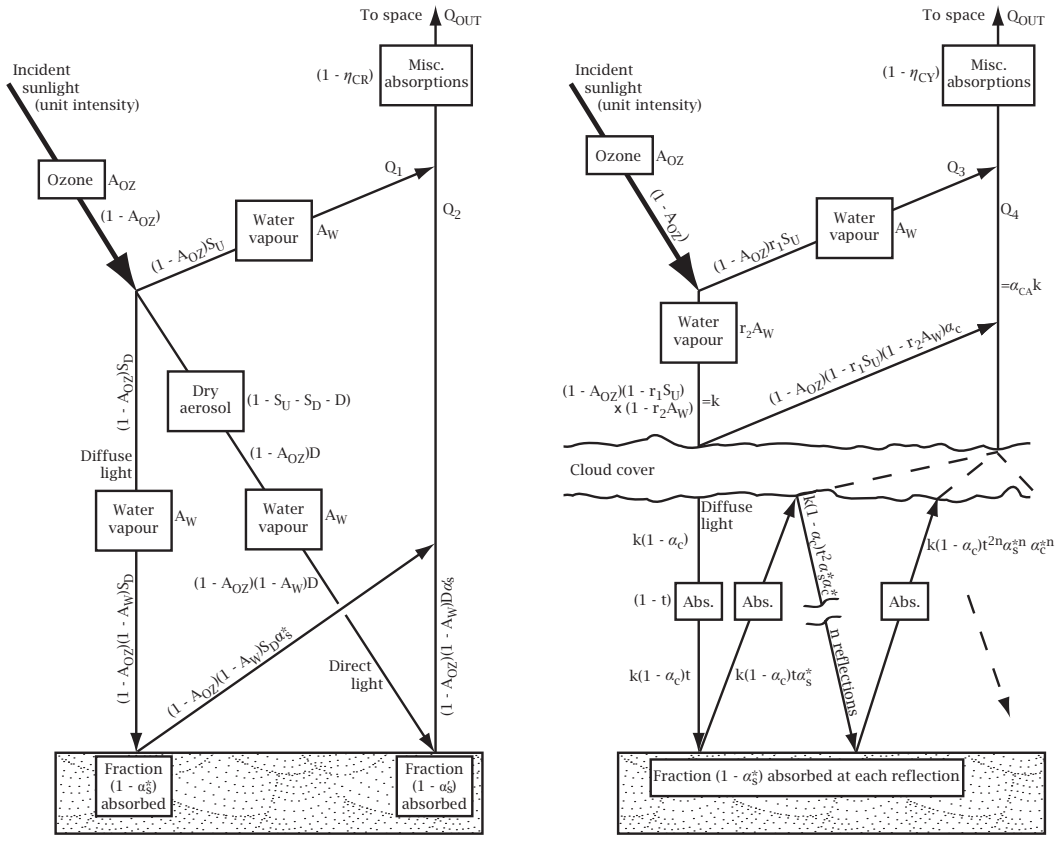

(a) Clear-skies case (b) Cloudy-skies case

Figure 20: Clear- and cloudy-skies shortwave schemes, based on .

For **clear skies**, the following equations apply with reference to Fig. 20 (a)[28]:

$$
\begin{aligned}
Q^{\star}_{A,CLEAR} &= Q_{OZONE} + Q_{VAPOUR} + Q_{DRY\,AER.} + Q_{MISC.} \qquad (42)\\
\text{with:}\quad Q_{OZONE} &= A_{OZ};\\
Q_{VAPOUR} &= (1 - A_{OZ})(S_U + S_D + D)A_W;\\
Q_{DRY\,AER.} &= (1 - A_{OZ})(1 - S_U - S_D - D);\\
Q_{MISC.} &= (1 - \eta_{CR})(Q_1 + Q_2) \quad \text{as marked on Fig. 20 (a)}\\
&= (1 - \eta_{CR})[(1 - A_{OZ})S_U(1 - A_W) +\\
&\qquad (1 - A_{OZ})S_D(1 - A_W)\alpha^{\star}_S +\\
&\qquad (1 - A_{OZ})D(1 - A_W)\alpha'_S];
\end{aligned}
$$

$$
\begin{aligned}
Q^{\star}_{S,CLEAR} &= Q_{DIFFUSE} + Q_{DIRECT} \qquad (43)\\
\text{with:}\quad Q_{DIFFUSE} &= (1 - A_{OZ})S_D(1 - A_W)(1 - \alpha'_S);\\
Q_{DIRECT} &= (1 - A_{OZ})D(1 - A_W)(1 - \alpha^{\star}_S)
\end{aligned}
$$

[28]Formulae for $S_U(Z)$,$S_D(Z)$ and $D(Z)$, the upward-scattered fraction, downward-scattered fraction, and the fraction remaining direct and not absorbed by dry aerosol, respectively, are given by Thompson and Barron. A formula to calculate $A_W(Z, T_A)$ is also given there; all other terms are constant.

For **cloudy skies**, the following equations apply with reference to Fig. 20 (b)[29]:

$$\begin{aligned} Q^{\star}_{A,\,CLOUDY} &= Q_{OZONE} + Q_{VAPOUR} + Q_{CLOUD} + Q_{MISC.} \qquad (44)\\ \text{with:}& \\ Q_{OZONE} &= A_{OZ};\\ Q_{VAPOUR} &= (1-A_{OZ})(1-r_1S_U)r_2A_W;\\ Q_{CLOUD} &= k(1-\alpha_{CA}) - Q^{\star}_S \quad \text{i.e. everything not reflected from clouds, minus } Q^{\star}_S\\ Q_{MISC.} &= (1-\eta_{CY})(Q_3+Q_4) \quad \text{as marked on Fig. 20 (b)}\\ & (1-\eta_{CY})[(1-A_{OZ})r_1S_U(1-A_W) + \alpha_{CA}(1-A_{OZ})(1-r_1S_U)(1-r_2A_W)] \end{aligned}$$

$$\begin{aligned} Q^{\star}_{S,\,CLOUDY} &= \sum\nolimits_{n=0}^{\infty} Q_{SURFACE,\,n} \quad \text{(energy absorbed at each surface reflection)} \qquad (45)\\ &= k(1-\alpha_C)t(1-\alpha^{\star}_S) + k(1-\alpha_C)t\alpha^{\star}_S.t\alpha^{\star}_C.t(1-\alpha^{\star}_S) +\\ &\qquad\qquad k(1-\alpha_C)t\alpha^{\star}_S.t\alpha^{\star}_C.t\alpha^{\star}_S.t\alpha^{\star}_C.t(1-\alpha^{\star}_S) + \ldots\\ &= kt(1-\alpha_C)(1-\alpha^{\star}_S)[1 + t^2\alpha^{\star}_S\alpha^{\star}_C + (t^2\alpha^{\star}_S\alpha^{\star}_C)^2 + \ldots]\\ &= kt(1-\alpha_C)(1-\alpha^{\star}_S)\sum\nolimits_{n=0}^{\infty}(\alpha^{\star}_S\alpha^{\star}_Ct^2)^n\\ &= \frac{kt(1-\alpha_C)(1-\alpha^{\star}_S)}{1-\alpha^{\star}_S\alpha^{\star}_Ct^2} = \frac{t(1-\alpha_C)(1-\alpha^{\star}_S)}{1-\alpha^{\star}_S\alpha^{\star}_Ct^2}(1-A_{OZ})(1-r_1S_U)(1-r_2A_W) \end{aligned}$$

The final absorptions are then calculated by multiplying the unit-intensity absorptions by the average intensity of incoming solar radiation, which is one quarter[30] of the incoming solar intensity of $P_{in} = 1373$ W m^{-2}: This gives overall absorptions of

$$\begin{aligned} Q^{\star}_{A,\,OVERALL} &= \tfrac{P_{in}}{4}\left[F_{CL}Q^{\star}_{A,\,CLOUDY} + (1-F_{CL})Q^{\star}_{A,\,CLEAR}\right]\\ Q^{\star}_{S,\,OVERALL} &= \tfrac{P_{in}}{4}\left[F_{CL}Q^{\star}_{S,\,CLOUDY} + (1-F_{CL})Q^{\star}_{S,\,CLEAR}\right] \end{aligned} \qquad (46)$$

where F_{CL} is the insolation- and area-weighted cloudy-skies fraction, equal to 0.531.

The final values yielded were very close to those given in Harvey and Schneider [9]: equations 46 give $Q^{\star}_A = 67.86$ W m^{-2} and $Q^{\star}_S = 165.45$ W m^{-2}, compared with Harvey and Schneider's $Q^{\star}_A = 66.90$ W m^{-2} and $Q^{\star}_S = 168.95$ W m^{-2}. The slight scaling was made in order to ensure that the equilibrium temperatures match theirs; note that this doesn't render the above process futile because we still need the functional variation with temperature given by (46).

[29] α_{CA} is the apparent cloud albedo, defined as $\alpha_C + (1-\alpha_C)[(1-t^2\alpha^{\star}_S\alpha^{\star}_C)^{-1} - 1]$. This is the albedo of the cloud as observed from above, taking into account reflections between the cloud and surface beneath. The formula is lifted directly from Thompson and Barron.

[30] The earth's surface area is given approximately $4\pi R^2$, and the radiation energy hitting the earth's profile is $P_{in}\pi R^2$, so the average intensity is $\frac{P_{in}\pi R^2}{4\pi R^2} = \frac{P_{in}}{4}$.

10 Glossary and Abbreviations

ACC (Active Climate Control): Human schemes intended to cause significant changes in the future global climate.
Albedo: Proportion of energy of incident radiation that is present in the reflected component. Denoted by α.
Biosphere: In this case, the carbon reservoir represented by the sum of all living and dead organisms.
CCS: Carbon Capture and Storage.
CDIAC: Carbon Dioxide Information Analysis Centre, part of the U.S. Department of Energy.
DIC (Dissolved Inorganic Carbon): Carbon present in oceans in dissolved compound. See footnote 5.
FFB: Fossil-fuel burning.
[AO]GCM ([Atmosphere-Ocean] General Circulation Model): Models which represent continuous variations and internal currents throughout climate components, e.g. the oceans and atmosphere.
GHG: Greenhouse gas.
Insolation: Intensity of incident solar radiation.
IPCC (Intergovernmental Panel on Climate Change): A body set up under the remit of the United Nations, which collates climate change research in order to inform government policy.
IR: Infrared.
LQR: Linear Quadratic Regulator.
PDE: Partial Differential Equation**.**
SAR: Second Annual Report from IPCC WGI.
SCM (Simple Climate Model): Simple models which parameterise complex and multi-dimensional climate effects down to a relatively small number of variables.
SWR: Shortwave radiation.
WGI (Working Group I): A subgroup of the IPCC which periodically releases reports on the scientific basis for climate policy.

References

[1] "The Great Global Warming Swindle". Channel 4 documentary, information at http://www.channel4.com/science/microsites/G/great_global_warming_swindle/.

[2] "The Sleipner West Field: Carbon Storage 1,000 Metres Down". Online article, http://www.statoil.com/co2.

[3] ANGEL, R. Feasibility of cooling the earth with a cloud of small spacecraft near the inner lagrange point. *Proc. Nat. Acad. Sci.* (Nov. 2006), 17184–17189.

[4] BERGER, A. L. Long-term variations of daily insolation and quaternary climatic changes. *J. Atmos. Sci. 35* (Dec. 1978), 2362–2367.

[5] BLACK, R. "Lovelock urges ocean climate fix". Online article, 26 Sep. 2007, http://news.bbc.co.uk/1/hi/sci/tech/7014503.stm.

[6] GIFFORD, R. M. Interaction of carbon dioxide with growth-limiting environmental factors in vegetation productivity: implications for the global carbon cycle. *Advances in Bioclimatology 1* (1992), 24–58.

[7] HARVEY, L. D. D. *Global Warming: The Hard Science*. Prentice Hall, 2000.

[8] HARVEY, L. D. D., AND HUANG, Z. A quasi-one-dimensional coupled climate-change cycle model (parts 1 and 2). *J. Geophys. Res. 106* (Oct. 2001), 22339–22372.

[9] HARVEY, L. D. D., AND SCHNEIDER, S. H. Transient climate response to external forcing on 10^0 to 10^4 year time scales: Part 1. *J. Geophys. Res. 90* (Feb. 1985), 2191–2205.

[10] HOLLAND, J. S. "The acid threat". Magazine article, Nov. 2007.

[11] HOUGHTON, J. *Global Warming: The Complete Briefing, 3rd Ed.* Cambridge Univ. Press, 2004.

[12] HOUGHTON, J. T., GYLVAN MEIRA FILHO, L., GRIGGS, D. J., AND MASKELL, K. An Introduction to Simple Climate Models used in the IPCC Second Assessment Report. Tech. rep., IPCC, Feb. 1997.

[13] IDSO, K. E., AND IDSO, S. B. Plant responses to atmospheric carbon dioxide enhancement in the face of environmental constraints: a review of the past 10 years' research. *Agricultural and Forest Meteorology 69* (1994), 153–203.

[14] LACIS, A. A., AND HANSEN, J. E. A parameterization for the absorption of solar radiation in the earth's atmosphere. *J. Atmos. Sci. 31* (Jan. 1974), 118–133.

[15] LACKNER, K. S., GRIMES, P., AND ZIOCK, H.-J. Capturing carbon dioxide from air. In *24th International Conference on Coal Utilization & Fuel Systems* (Clearwater, FL, USA, 8-11 Mar. 1999), pp. 885–896.

[16] LAUNDER, B. E. Geo-engineering for Climate Stabilisation: Public lecture, City University, London, 3 Apr. 2008.

[17] LOVELOCK, J. E., AND RAPLEY, C. G. "Ocean pipes could help the earth cure itself". Correspondence, Nature 26 Sep. 2007.

[18] LOWE, P. R. An approximating polynomial for the computation of saturation vapor pressure. *J. Appl. Meteor. 10* (1976), 100–103.

[19] MARTIN, J. H., AND FITZWATER, S. E. Iron-deficiency limits phytoplankton growth in the northeast pacific subarctic. *Nature 331* (28 Jan. 1988), 341–343.

[20] MCCARTHY, M. "Pipes hung in the sea could help the planet to 'heal itself'". Newspaper article, The Independent, 27 Sep. 2007.

[21] MICHAELSON, J. Geoengineering: a climate change Manhattan Project. *Stanford Environmental Law Journal 17:1* (Jan. 1998).

[22] NAKICENOVIC, N., AND GROUP. IPCC Special Report on Emissions Scenarios. Tech. rep., IPCC, 2000.

[23] OESCHGER, H., SIEGENTHALER, U., SCHOTTERER, U., AND GUGELMANN, A. A box diffusion model to study the carbon dioxide exchange in nature. *Tellus 27* (Jun. 1975).

[24] RAMANATHAN, V. Interactions between ice-albedo, lapse-rate and cloud-top feedbacks: An analysis of the nonlinear response of a GCM climate model. *J. Atmos. Sci. 34* (1977), 1885–1896.

[25] RAMASWAMY, V., AND GROUP. Climate Change 2001: Working Group I: The Scientific Basis. Tech. rep., IPCC, 2001.

[26] RAMPINO, M. R., AND SELF, S. Historic eruptions of Tambora (1815), Krakatau (1883), and Agung (1963), their stratospheric aerosols, and climatic impact. *Quaternary Research 18* (Sep. 1982), 127–143.

[27] RAVEN, J., AND GROUP. Ocean acidification due to increasing atmospheric carbon dioxide. Tech. rep., The Royal Society, Jun. 2005.

[28] RITTER, M. E. *The Physical Environment: an Introduction to Physical Geography*. University of Wisconsin Stevens Point, 2006.

[29] ROBOCK, A., OMAN, L., AND STENCHIKOV, G. L. Nuclear winter revisited with a modern climate model and current nuclear arsenals: Still catastrophic consequences. *J. Geophys. Res. 112* (Jul. 2007).

[30] SALTER, S., SORTINI, G., AND LATHAM, J. Sea-going hardware for the cloud albedo method of reversing global warming. *Draft preprint for Phil. Trans. Roy. Soc.* (2008).

[31] SARMIENTO, J. L., AND BRYAN, K. An ocean transport model for the North Atlantic. *J. Geophys. Res. 87* (Jan. 1982), 394–409.

[32] SCHMALENSEE, R., STOKER, T. M., AND A., J. R. World carbon dioxide emissions: 1950-2050. *The Review of Economics and Statistics 80:1* (Feb. 1998), 15–27.

[33] SELLERS, W. D. *Physical Climatology*. Chicago University Press, 1965.

[34] SOLOMON, S., QIN, D., MANNING, M., AND GROUP. Climate Change 2007: The Physical Science Basis. Tech. rep., IPCC, 2007.

[35] STERN, N. *The Economics of Climate Change: The Stern Review*. 2006.

[36] TELLER, E., HYDE, R., AND WOOD, L. "Active Climate Stabilization: Practical Physics-Based Approaches to Prevention of Climate Change"; Presentation at the National Academy of Engineering Symposium Complements to Kyoto: Technologies for Controlling CO_2 Emissions, National Academy of Sciences, 23-24 Apr. 2002.

[37] THOMPSON, S. L., AND BARRON, E. J. Comparison of Cretaceous and present earth albedos: Implications for the causes of paleoclimates. *J. Geol. 89* (Mar. 1981), 143–167.

[38] TYNDALL CENTRE, CAMBRIDGE-MIT INSTITUTE SYMPOSIUM. Macro-engineering Options for Climate Change Management and Mitigation: Summary Report, 7-9 Jan. 2004.

[39] UPSON, S. "Algae bloom climate-change scheme doomed": Magazine article, IEEE Spectrum, Jan. 2008.

Acknowledgment

Many thanks to my supervisor, Prof Malcolm Smith, for his patience as many a meeting overran. Thanks are also due for inviting me to represent him at the Edwards Lecture [16] at City University in April, from which fresh inspiration for the project was drawn. Thanks to Dr Jorge Gonçalves for his feedback on previous parts of the project.

Risk Assessment Retrospective

As required, this section details any changes to the risk assessment for this project that would be made in retrospect. Since the only tools used were computers, no new measures aside from those given in the original assessment for the prevention of RSI and eye strain need be considered.